

UNIVERSITY OF TWENTE.

Faculty of Science & Technology

**Model-based wavefront shaping
to improve imaging
in lung-on-a-chip devices**

Merle van Gorsel

S1883925

M.Sc. Thesis Applied Physics

February 2021

Supervisors:

prof. dr. ir. I. M. Vellekoop

prof. dr. ir. S. Le Gac

dr. R. Saive

dr. ir. A. Thendiyammal

Biomedical Photonic Imaging Group

ABSTRACT

Organ-on-a-chip devices can offer a human cell-based model to improve the drug development process. The geometry and composition of materials of the chip make it difficult to image ongoing biological processes, because light is aberrated by the sample. Light cannot form a focus, which results in a poor image quality.

In this research, model-based wavefront shaping is investigated as a method to improve the focus inside two lung-on-a-chip samples. A two-photon microscope is used to obtain a stack of images of the interface that causes aberrations. These images are used to reconstruct a digital model of the refractive index distribution of the sample. This digital refractive index model is used to perform a virtual phase conjugation experiment. We simulate the propagation of light from a virtual point source through the refractive index model of the sample to find the aberrated field. If the phase conjugate of the aberrated field is propagated back through the sample, the light forms a focus at the position of the virtual point source due to the time-reversal nature of light.

By making a simulation of the virtual phase conjugation experiment, we calculated a theoretical maximum increase in intensity of 3.2x. In a proof of concept experiment using a PDMS sample, we achieved a 1.8x increase of intensity in a bulk of fluorescein inside the sample. Based on these results, we proceeded with a sample containing a collagen matrix in which epithelial cells can be grown. We managed to reconstruct a refractive index distribution without labelling, using the second-harmonic properties of collagen. The simulations predict a 169x increase in intensity for this sample when used in an experiment. Due to time constraints, this has not been experimentally confirmed yet.

Contents

Abstract	1
1 Introduction	3
2 Theory	6
2.1 Beam propagation method	6
2.2 Modeling light propagation through the samples	7
2.2.1 PDMS sample	7
2.2.2 Collagen sample	9
2.3 Simulation of the virtual phase conjugation experiment	10
2.3.1 Quantifying the simulated enhancement of the focus	10
2.3.2 PDMS sample	12
2.3.3 Collagen sample	17
3 Experimental	22
3.1 Setup	22
3.2 Sample preparation	23
3.3 Measurement procedure	23
4 Experimental results	25
4.1 Experimental results: PDMS sample	25
4.2 Experimental results: collagen sample	29
5 Conclusion and recommendations	31
Bibliography	32
A Protocol: Imaging lung-on-a-chip with TPM	33
B Fabrication of microfluidic chips for the lung-on-chip project	39
C Collagen hydrogel preparation	41
D Protocol: Polydopamine coating	44

1 INTRODUCTION

The development of a new drug is a timely and costly process, and most drugs that enter the clinical trials never make it to the marketplace. Conventional drug testing often relies on cell culture models, which cannot express tissue-specific functions [1]. Organ-on-a-chip devices can provide a human cell-based model of an organ, which replicates the response on a drug more accurately than conventional cell cultures [2] or animals.

However, the geometry and composition of materials of the chips make it difficult to image ongoing biological processes. When light travels through the chip, refraction and aberrations due to the geometry of the sample prevent the light from forming a focus. In order to image the chip, the researcher has to terminate the experiment to disassemble the chip for imaging. This makes it impossible to gather real-time information on biological processes.

In this thesis, we investigate the use of optical wavefront shaping for imaging inside organ-on-a-chip devices. Wavefront shaping is a technique where the phase of the incoming light beam is modulated to counteract scattering, so a focus can be created in a scattering medium, as illustrated in Fig. 1.1. A smaller focus means that smaller features can be resolved, and therefore results in a higher imaging resolution. Conventional methods of wavefront shaping often rely on the feedback signal directly at the focus location [3] or from a guide star to find the correction wavefront [4]. Inserting a guide star in a sample is not always feasible and the correction wavefront is only applicable to a small region outside the guide star due to the optical memory effect [5]. Therefore, the applications of feedback-based wavefront shaping are limited.

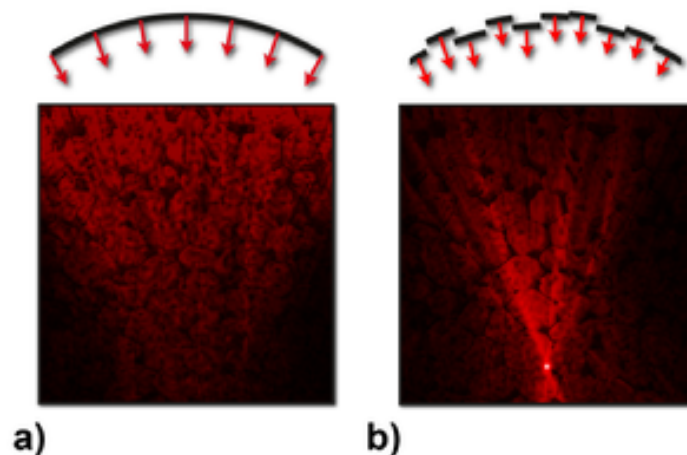


Figure 1.1: Principle of wavefront shaping. a) A spherical wavefront is incident on a scattering medium. Light is scattered and does not converge inside the medium. b) By adjusting the phase of the incident wavefront, a focus is made inside the scattering medium. Image reproduced from [6].

In 2020, a new type of wavefront shaping was introduced, called model-based wavefront shaping microscopy [7]. This method numerically computes the optimal wavefront to correct for aberrations introduced by the sample. The concept of model-based wavefront shaping is illustrated in Fig. 1.2. A two-photon microscope (TPM) is used to obtain a stack of images of the surface of the sample where light is scattered. This stack of images is used to reconstruct a refractive index model of the surface of the sample. The surface of the sample was visualized using fluorescein dye. In the second step, the refractive index model of the sample is used to calculate the wavefront correction. This is done by performing a virtual optical phase conjugation experiment. Optical phase conjugation, also known as time reversal, means that for any solution to an equation that contains time-reversal symmetry, there exists a solution with the reversed time that is also a solution to that equation [8]. The propagation of light is described by the electromagnetic wave equation, which contains time-reversal symmetry because they are derived from the Maxwell equations. The solution to forming a focus inside an aberrating sample can be found by reversing the wave resulting from a point source in the sample. For a monochromatic field, time reversal is equivalent to a sign reversal of the phase, which is known as the phase conjugate. In the third step, we take the phase conjugate of the calculated aberrated field and place it on a spatial light modulator (SLM). As the conjugated field propagates through the sample, it forms a sharp focus at the location where the virtual point source was placed in the model.

Model-based wavefront shaping has already outperformed conventional wavefront shaping by a factor of two in imaging depth and resulted in a 21-fold increase in intensity at the deepest optimized point [7].

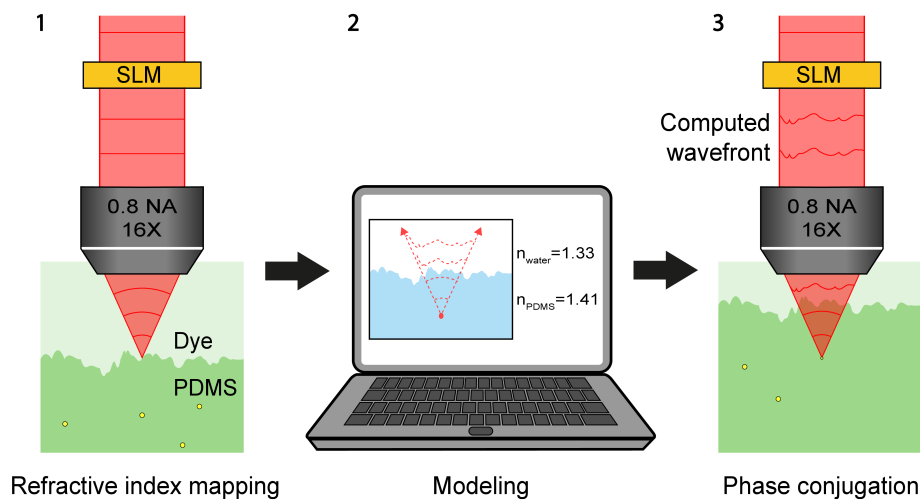


Figure 1.2: The three steps of model-based wavefront shaping: 1) two-photon excitation microscopy (TPM) is used to reconstruct a digital model of the refractive index distribution of the sample from the image data. 2) The refractive index distribution model is used to compute the wavefront to form a focus at a desired location in the sample. 3) The computed wavefront is phase conjugated and constructed by a spatial light modulator to compensate the aberration of light and to form a focus inside the medium. Image reproduced from [7].

This research explores the application of model-based wavefront shaping for improving imaging inside lung-on-a-chip devices. For the first time ever, a 3D-model of the refractive index distribution of the sample is used instead of a 2D interface. In state-of-the-art research, the scattering surface of the sample was imaged using fluorescein dye to visualize the surface. In this research, the aberrating surface is imaged within the sample without use of additional staining, by making use of the second harmonic properties of collagen. A TPM is used to obtain a stack of images of the aberrating surface inside the sample. From this stack of images, a

refractive index distribution of the boundary is reconstructed using a *a priori* knowledge about the materials in the sample. The layer thicknesses of the different refractive index materials of the sample are measured using the TPM. The reconstructed refractive index distribution of the boundary and the measured layer thicknesses are combined to construct a digital refractive index model of the sample.

The samples used during this research are culturing devices to grow artificial lung tissue, provided by the Applied Microfluidics for BioEngineering Research (AMBER) group at the University of Twente. These chips are designed to investigate the uptake of nanometer-sized plastic particles by lung epithelial cells. A simplified illustration of the sample is presented in Fig. 1.3a.

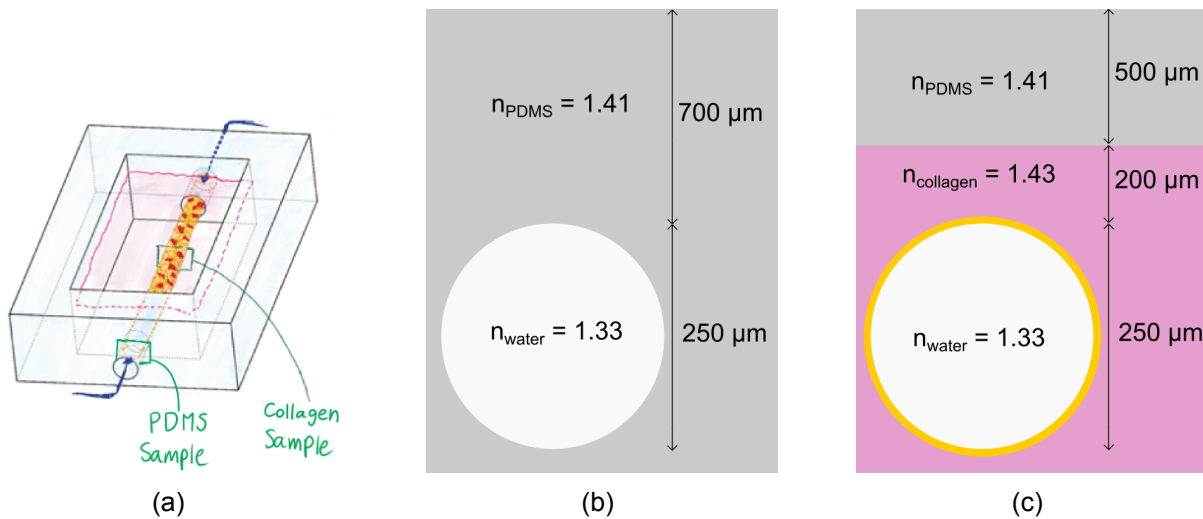


Figure 1.3: (a) Schematic drawing of the geometry of the chip. The epithelial cells are grown on the inside of a hollow tube of collagen. Image provided by AMBER group. (b) Illustration of a cross-section of the PDMS sample (c) Illustration of a cross-section of the collagen sample. Epithelial cells are indicated by the yellow ring around the tube.

The structure of the chip is made of polydimethylsiloxane (PDMS), with a central reservoir filled with collagen. Through the length of a chip lies a hollow cylinder with a diameter of $250\ \mu\text{m}$, which for the remainder of this report will be referred to as “the tube”. In the central reservoir of the chip, epithelial lung cells are grown on the inside of the tube, indicated with the yellow ring in Fig. 1.3c.

During this research we imaged two regions of the chip:

1. The part of the chip where the tube is surrounded by only PDMS. This part of the chip will be referred to as the “PDMS sample”, cross-section illustrated in Fig. 1.3b.
2. The part where the tube is situated in the central reservoir of the sample. The tube is surrounded by collagen with a layer of PDMS below it. The inside of the hollow tube is covered with epithelial cells with FITC stained nanoplastics. This part of the chip will be referred to as the “collagen sample”, cross-section illustrated in Fig. 1.3c.

In Chapter 2 we explain the theory behind modeling the light propagation through the sample. After that, we discuss the modeling steps we perform to calculate the correction wavefront. We performed a simulation of the phase conjugation experiment to calculate the theoretical enhancement of model-based wavefront shaping for the samples. We simulate the focus before and after using wavefront shaping and compare the results based on the maximum intensity in the focus and the width of the focus. Chapter 3 presents the experimental setup and the measurement procedure used during the experiment. In Chapter 4 we present the results of the experiment for both the PDMS sample and the collagen sample. In Chapter 5 we form our conclusions and present recommendations for further research.

2 THEORY

In this chapter we explain how the light propagation is modeled through the samples. The digital refractive index model of the sample is divided into simulation volumes. Section 2.1 explains the beam propagation method that is used to calculate the propagation of light through a simulation volume. Section 2.2 is divided into two subsections. Subsection 2.2.1 explains the steps to calculate the correction wavefront for a virtual point source located in the center of the tube in the PDMS sample. Subsection 2.2.2 explains the modeling steps for the propagation of light of a virtual point source located at the bottom of the tube in the collagen sample.

2.1 Beam propagation method

The digital refractive index model of the sample is divided into simulation volumes for ease of modelling. To simulate light propagation through each simulation volume of thickness d_x , we use a beam propagation method [9], based on the angular spectrum method [10]. Consider the field $E(x, y, z)$ of a monochromatic light source, which propagates through a medium of refractive index n over a distance d_x in the positive z direction as illustrated in Fig. 2.1. The goal is to calculate the field $E(x, y, z + d_x)$ after propagating a total distance d_x through the simulation volume. To do this, we Fourier transform the field $E(x, y, z)$ to analyze the field as a superposition of plane waves, $E(k_x, k_y, k_z)$. The distance d_x is split up into a number of infinitesimally thin phase plates with spacing b to approximate the 3D distribution of the medium the field travels through. The propagation over a distance b is modelled as a multiplication with the term $\exp(ik_z b)$ with $k_z = \sqrt{(\langle n \rangle k_0)^2 - k_x^2 - k_y^2}$ where $\langle n \rangle$ is the average refractive index of the slice. The result after propagating a distance b is the field $E(k_x, k_y, k_z + b)$. We use the inverse Fourier transform to transform back to the spatial domain to get $E(x, y, z + b)$, taking into account the phase shifts the waves encounter upon propagation. This procedure is repeated until the total distance d_x of the simulation volume is traveled.

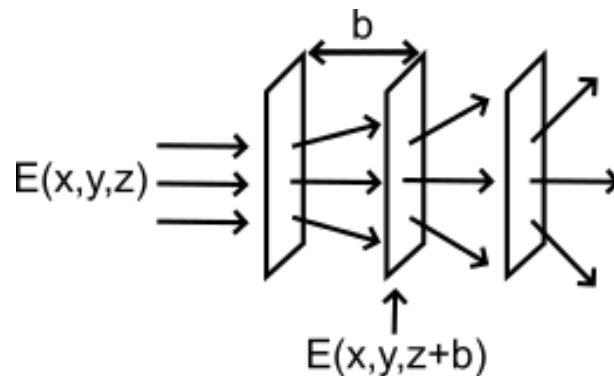


Figure 2.1: Illustration of the beam propagation method. Image inspired by [11].

2.2 Modeling light propagation through the samples

This section explains how the beam propagation method is applied to model light propagation through the sample. To keep the calculation manageable, we only consider aberrations introduced by the sample and neglect aberrations caused by the optical components in the setup. Since the samples have a different composition of materials, their refractive index models are each divided into a number of simulation volumes fitting to their design. This section is therefore split into subsection [2.2.1](#) and [2.2.2](#) to separately discuss the modeling of light propagation through the PDMS sample and the collagen sample respectively.

2.2.1 PDMS sample

Figure [2.2](#) illustrates a cross-section of the PDMS sample, where a virtual point source is placed in the center of the tube. The propagation of light from the point source towards the outside of the sample is drawn with blue lines. To model the light propagation through the sample, the model is divided into five simulation volumes.

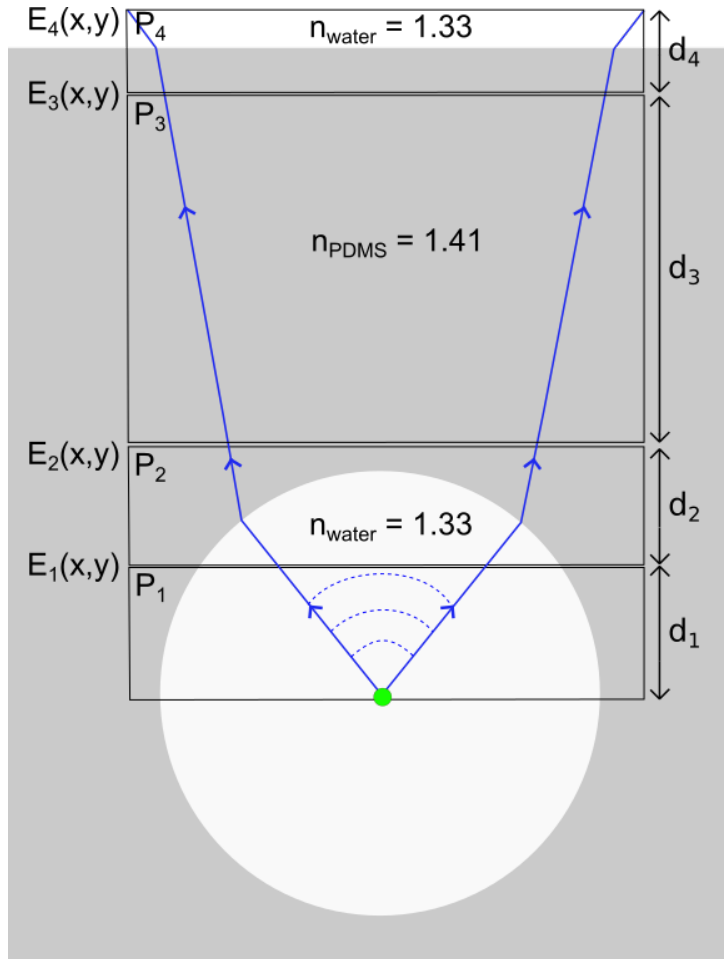


Figure 2.2: Illustration of the cross-section of the PDMS sample. Modeling the light propagation towards the surface of the sample is divided into five simulation volumes, indicated by the black rectangular regions.

1. We analytically generate a spherical wavefront from a point source a distance d_1 from plane P_1 . The field $E_1(x, y)$ at plane P_1 has the form:

$$E_1(x, y) = E_0 \exp \left(i \frac{2\pi n_{water}}{\lambda} \left[\sqrt{d_1^2 + x^2 + y^2} - |d_1| \right] \right), \quad (2.1)$$

where n_{water} is the refractive index of water, λ is the wavelength of the light, d_1 is the distance from the point source to plane P_1 , x and y are the spatial coordinates of the electric field. The maximum angle of light emerging from the point source is set to correspond with the numerical aperture of the microscope objective.

2. The beam propagation method is used to propagate the field $E_1(x, y)$ through the reconstructed refractive index distribution of the upper part of the tube. The procedure of the reconstruction is explained in Section 4.1. The refractive index distribution with a thickness of 50 μm is divided into 150 equally-spaced infinitely thin phase plates to approximate the 3D distribution of the sample. The electric field after propagation, $E_2(x, y)$, is located at plane P_2 .
3. We assume the field $E_2(x, y)$ propagates over a distance d_3 through PDMS without scattering. After propagation, the field $E_3(x, y)$ is found at plane P_3 .
4. The PDMS-water interface of the top of the sample is assumed to be flat. Therefore, the PDMS-water interface is modeled as a 15 μm layer of PDMS and a 15 μm layer of water, making the total thickness of this simulation volume 30 μm . The resulting computed field $E_4(x, y)$ is located at plane P_4 .
5. The last step to calculating the correction wavefront is to propagate the aberrated field $E_4(x, y)$ to the plane of the SLM. To propagate the field to the SLM, we would have to simulate the light propagation through the optical components of the setup to the position of the SLM. This process greatly increases the computation time, so instead we propagate the field back to the image plane of the microscope objective. If we assume that the microscope objective is a perfect lens, then the field in the focal plane and the field at the pupil plane are a Fourier pair. This way, once we have propagated the field to the image plane, we can use a Fourier transformation to put the field on the SLM.

To compare the foci made with and without using a correction, the foci must be at the same position in the sample. We propagate the field $E_4(x, y)$ over a distance

$$d_{SLM} = d_1 + d_2 + \frac{n_{PDMS}}{n_{water}}(d_3 + \frac{d_4}{2}) + \frac{d_4}{2} \quad (2.2)$$

to the image plane of the microscope objective to get $E_{SLM}(x, y)$. Because the microscope objective is designed to be water immersed, we multiply the thickness of each simulation volume with their refractive index relative to water. The field $E_{SLM}(x, y)$ is Fourier transformed to obtain $E_{SLM}(k_x, k_y)$ which is put at the SLM to enhance the focus inside the sample.

2.2.2 Collagen sample

Figure 2.3 is an illustration of a cross-section of the collagen sample, where the tube is surrounded by collagen with a layer of PDMS above it. In this sample, the walls of the tube contain epithelial lung cells with FITC stained 100 nm nanoplastics. The virtual point source is placed on the bottom of the tube, to enhance the focus at the position of the stained nanoplastics. To model the light propagation through the sample, the model is divided into six simulation volumes. Since many modeling steps are the same for both samples, only the differences with respect to modeling steps for the PDMS sample are discussed.

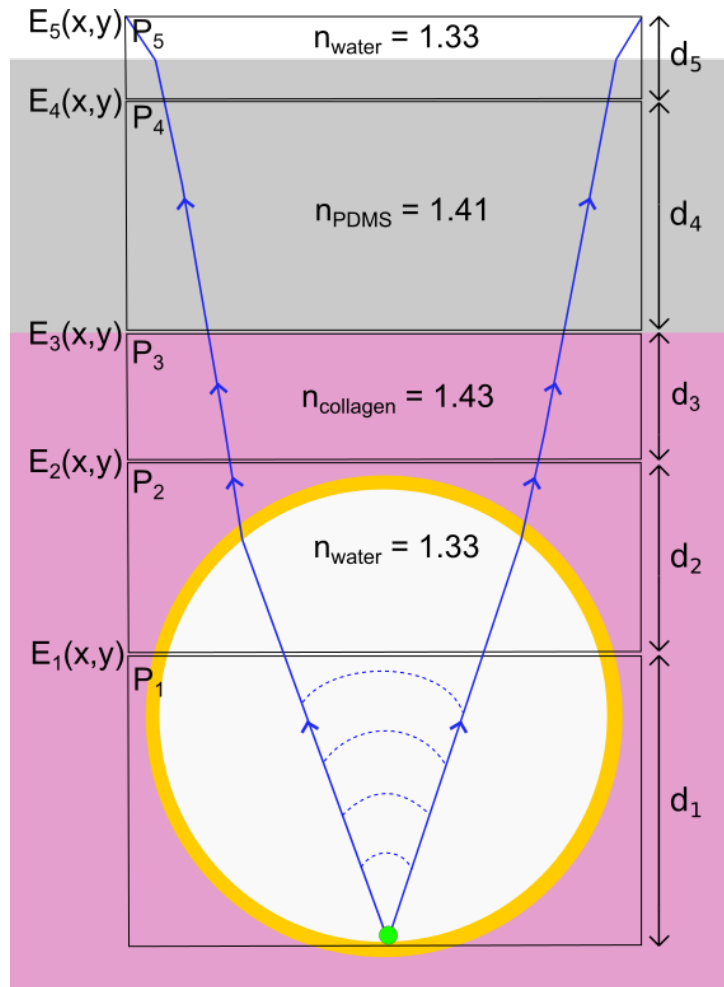


Figure 2.3: Illustration of the cross-section of the tube in collagen. A virtual point source is placed at the bottom of the tube. To model the light propagation through the sample, the model is divided into six simulation volumes.

1. The first step is the same as for the PDMS sample, the only difference being the distance d_1 . Since the point source is placed at the bottom of the tube, this distance is larger than in the case of the PDMS sample.
2. Because the distance d_1 is larger than for the PDMS sample, the size of $E_1(x, y)$ is larger as well. This means that the reconstructed refractive index distribution must include more of the curvature of the tube to propagate $E_1(x, y)$ through it. The refractive index distribution has a thickness of 150 μm and is divided into 350 equally-spaced infinitely thin phase plates. The reconstruction of the refractive index distribution is explained in Section 4.2.

3. We model the propagation of $E_2(x, y)$ over a distance d_3 through collagen. We assume the collagen to be a non-scattering medium.
4. The field $E_3(x, y)$ propagates over a distance d_4 through PDMS without light aberration. The computed field is found at plane P_4 .
5. The PDMS-water interface of the top of the sample is modeled the same as for the PDMS sample. The resulting computed field $E_5(x, y)$ is located at plane P_5 .
6. The last step to calculating the correction wavefront is to propagate the phase conjugate of the aberrated field $E_5(x, y)$ to the plane of the SLM. The field $E_5(x, y)$ is propagated over a distance

$$d_{SLM} = d_1 + d_2 + \frac{n_{PDMS}}{n_{water}} \left(d_3 + \frac{d_5}{2} \right) + \frac{n_{collagen}}{n_{water}} d_4 + \frac{d_5}{2} \quad (2.3)$$

to the image plane of the microscope objective to get $E_{SLM}(x, y)$. The field $E_{SLM}(x, y)$ is Fourier transformed to obtain $E_{SLM}(k_x, k_y)$ which is put at the SLM to enhance the focus inside the sample.

2.3 Simulation of the virtual phase conjugation experiment

In the previous section we explained the method used to find the correcting wavefront. In this section, we want to predict how much the focus should improve. To do so, we performed a simulation of the virtual phase conjugation experiment for the PDMS sample and the collagen sample. To quantify how well wavefront shaping works, we compare the width of the focus and the maximum intensity in the focus for three situations:

- The ideal situation, without aberrations
- With aberrations introduced by the sample
- Correcting for the aberrations introduced by the sample using wavefront shaping

2.3.1 Quantifying the simulated enhancement of the focus

The enhancement is quantified by inspecting the width of the focus, which is defined as the FWHM of the intensity distribution at a cross-section through the point with the maximum intensity. The FWHM of the intensity distributions is used to determine the lateral resolution of the system based on the Rayleigh criterion [12] [13] illustrated in Fig. 2.4. The Rayleigh criterion states that two points of equal intensity can be just resolved when the maximum of the first point falls on the minimum of the second point, as illustrated in Fig. 2.4b. If two points are closer to each other than the FWHM of the cross-section of the focus, the two points cannot be resolved, see Fig. 2.4a.

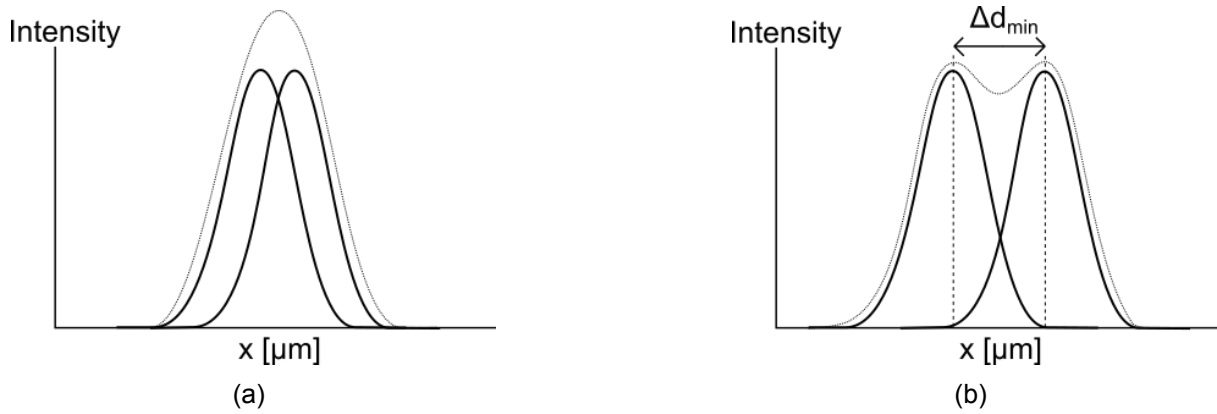


Figure 2.4: (a) Two points that are closer together than the FWHM of the focus cannot be resolved (b) Two points are just resolved when the peaks are separated by a distance Δd_{\min} . This minimum distance Δd_{\min} between the two peaks equals the FWHM of the cross-section of the focus.

The quality of the focus is expressed by the “Strehl ratio”, which is defined as the ratio of the maximum intensity of the actual point spread function to the perfect point spread function of a diffraction limited system [14]. The Strehl ratio is a number between 0 and 1 and measures how close the imaging system is to the diffraction limit. A system without any aberration has a Strehl ratio of 1, but an optical system with a Strehl ratio greater than 0.8 is generally considered diffraction-limited for practical purposes [14]. For the perfect point spread function, we simulated the converging beam of the microscope objective in water, since this is the smallest attainable focus.

For both samples, we calculated two Strehl ratios:

- **Strehl ratio of the system before applying the correction:** The ratio between the maximum intensity of the focus made with a converging spherical wavefront to a perfect point spread function

$$S_{\text{before}} = \frac{I_{\text{before}}}{I_{\text{perfect}}} \quad (2.4)$$

This ratio is expected to be low, because light is aberrated by the sample and the focus will be distorted.

- **Strehl ratio of the system after applying the correction:** The ratio between the maximum intensity of the focus made with the correction wavefront to a perfect point spread function

$$S_{\text{after}} = \frac{I_{\text{after}}}{I_{\text{perfect}}} \quad (2.5)$$

It is expected that S_{after} has a higher value than S_{before} , because we use the correction wavefront to correct for the aberrations induced by the sample. By comparing S_{before} to S_{after} , we determine how much the intensity in the focus has improved.

2.3.2 PDMS sample

Simulating spherical wavefront through the PDMS sample

We first simulate the focus made without applying a correction. The spherical wavefront has an opening angle corresponding to the opening angle of the microscope objective. The reconstructed refractive index distribution of the tube used in this simulation is shown in Fig. 4.3b. We improve the focus at a depth of 892 μm below the surface of the sample. The dashed box in Fig. 2.5 indicates the region in the sample that is investigated.

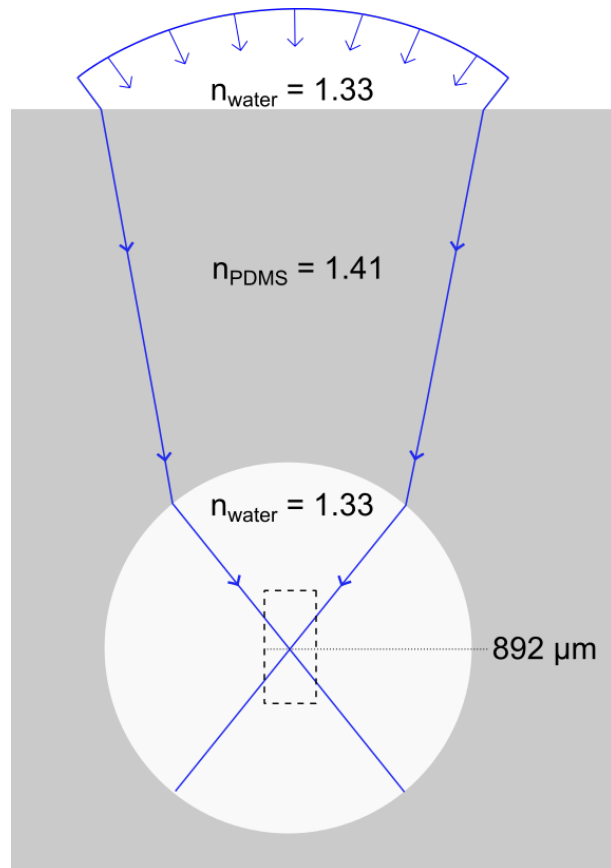


Figure 2.5: Illustration of the cross-section of the PDMS sample. The dashed box indicates the region in the sample shown in Fig. 2.6.

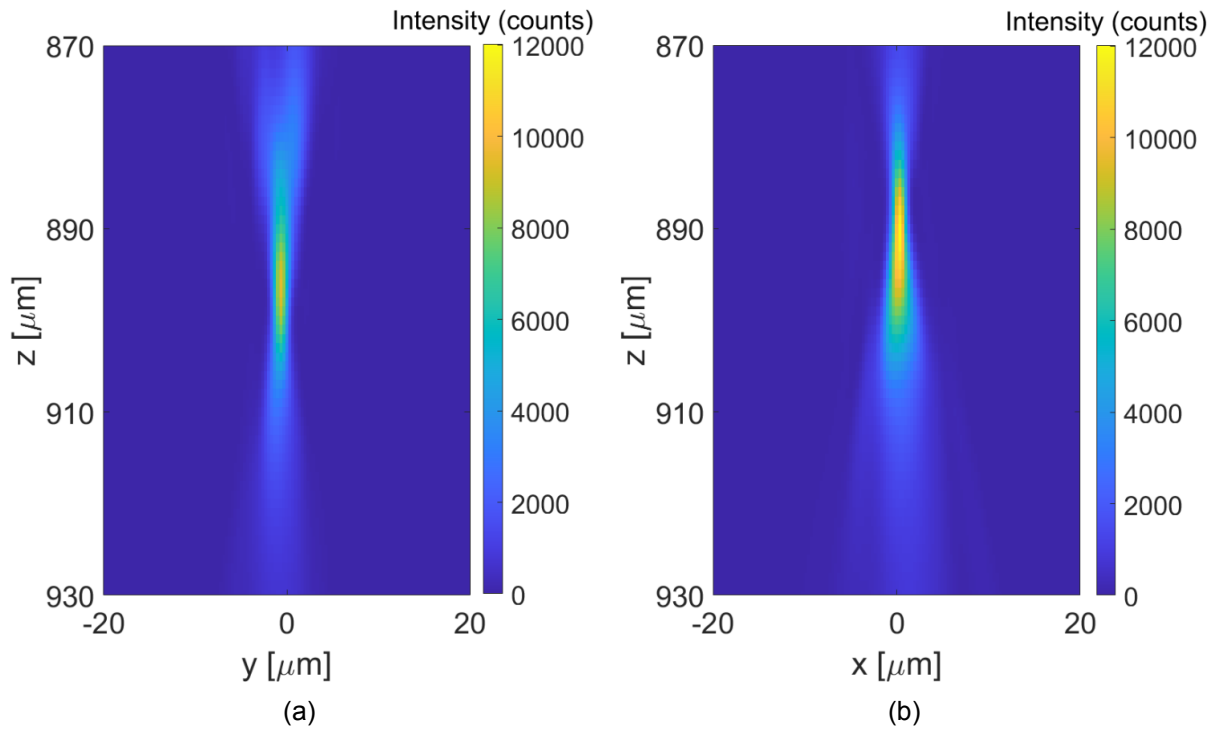


Figure 2.6: Cross-section of simulating the propagation of a spherical wavefront through the PDMS sample to form a focus in the center of the tube. The circle of least confusion is found at $892 \mu\text{m}$ below the surface of the sample (a) yz plane (b) xz plane.

Figure 2.6 shows cross-sections of the focus made by simulating the propagation of the spherical wavefront through the PDMS sample. When we compare Fig. 2.6a and 2.6b, it can be noticed that the position of the focus is different for both planes. This effect is called astigmatism, which is caused by the cylindrical shape of the tube. The foci for the yz and xz planes are found at $895 \mu\text{m}$ and $889 \mu\text{m}$ below the surface, respectively. The highest intensity is found at the smallest cross-section of the beam, which is called the circle of least confusion. The circle of least confusion is found at a depth of $892 \mu\text{m}$ below the top surface of the sample. This system has a lateral resolution of $1.85 \mu\text{m}$ based on the FWHM of the green solid curve shown in Fig. 2.10. The Strehl ratio of the system before applying wavefront shaping is calculated to be $S_{\text{before}} = 0.49$.

Simulating virtual phase conjugation experiment through the PDMS sample

We follow the modeling steps described in subsection 2.2.1 to calculate the aberrated field $E_4(x, y)$. The virtual point source is placed at the depth where we found circle of least confusion, 892 μm below the surface of the sample. We model the light propagation through the sample towards plane P_4 to find the phase of the correction wavefront, shown in Fig. 2.7.

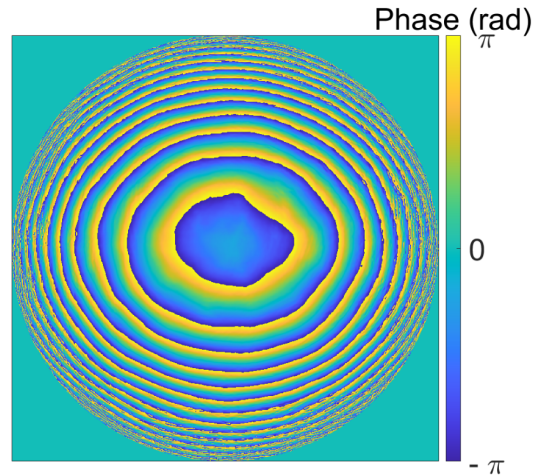


Figure 2.7: The calculated correction wavefront to focus light in the center of the tube of the PDMS sample. The size of the circle corresponds to the pupil of an objective with NA = 0.8.

To simulate the focus using the correction wavefront, we take the phase conjugate of the aberrated field $E_4(x, y)$ and propagate it back through the sample. Figure 2.8 shows a cross-section of the focusing beam, as a result of propagating the correction wavefront through the PDMS sample.

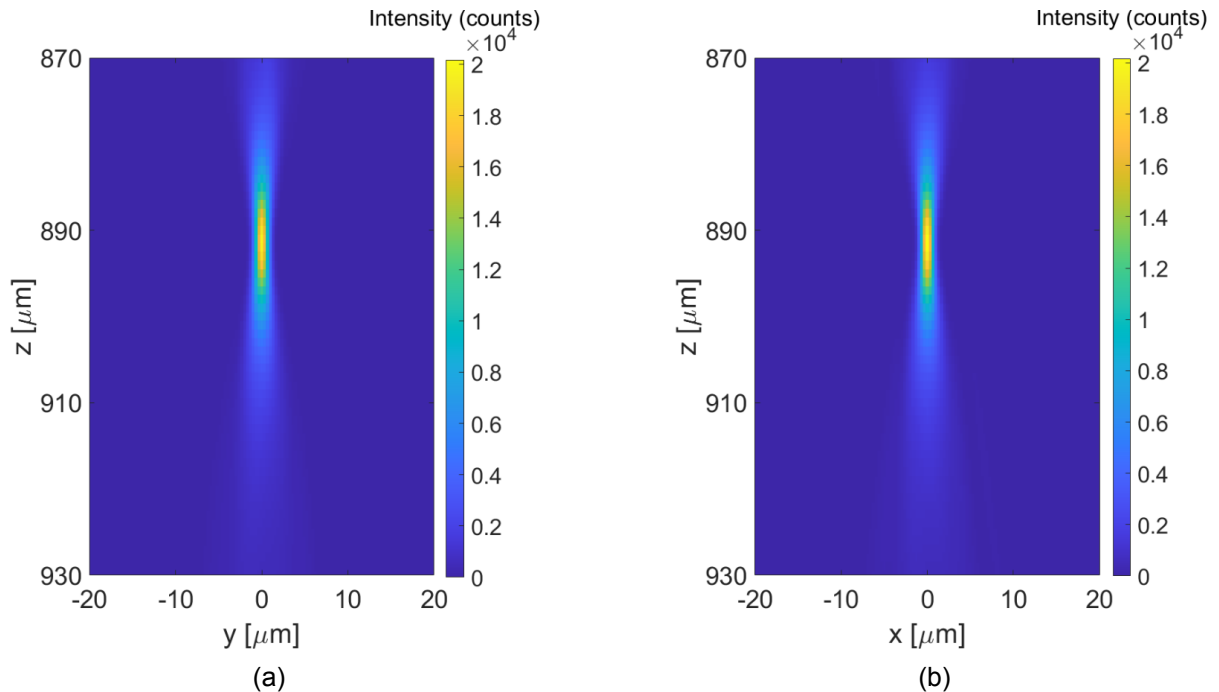


Figure 2.8: Result of simulating the focus made with the calculated correction wavefront through the PDMS sample. Cross-section of the beam propagating through the PDMS sample to form a focus at 892 μm below the surface of the sample (a) yz plane (b) xz plane.

When we compare figure 2.6 and 2.8, we notice an improvement of the maximum intensity in the focus. In Fig. 2.6 we defined the circle of least confusion at $892 \mu\text{m}$, because astigmatism caused light to focus at $895 \mu\text{m}$ and $889 \mu\text{m}$ inside the sample. In Fig. 2.8, we see that the light is focused at $892 \mu\text{m}$ for both imaging planes. This means that the correction wavefront has corrected for astigmatism caused by the tube. For the imaging system with wavefront shaping, we calculate a lateral resolution of $1.33 \mu\text{m}$ using the FWHM of the red dashed curve in Fig. 2.10. For the system with wavefront shaping we calculate a Strehl ratio of $S_{\text{after}} = 0.92$.

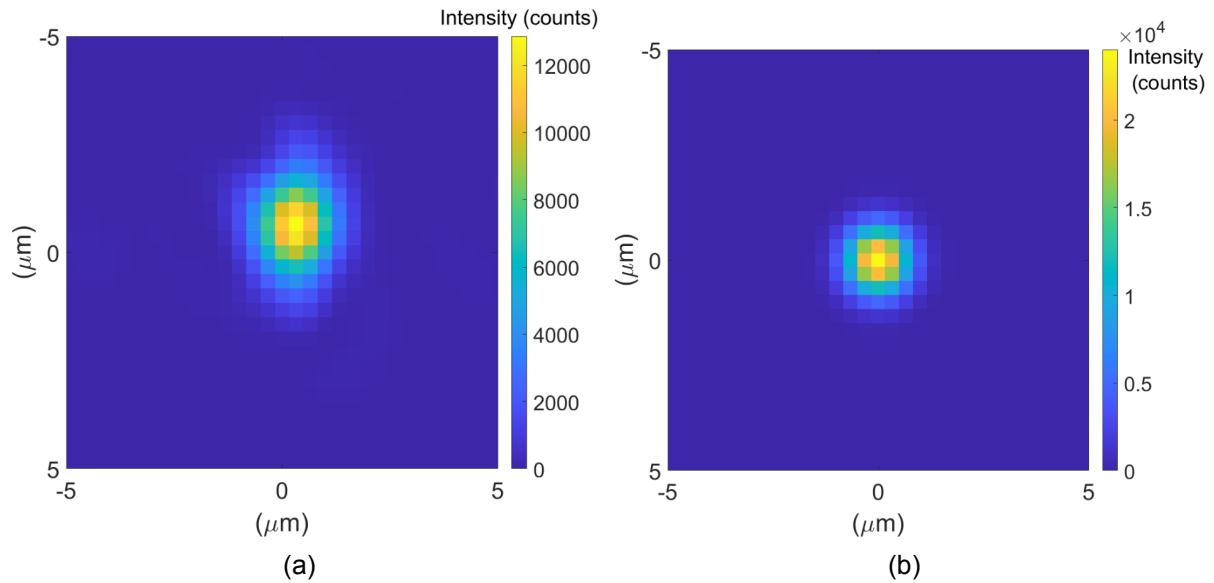


Figure 2.9: Simulation of the cross-section of (a) the circle of least confusion made by a spherical wavefront (b) the focus made by correction wavefront. The focus made with the correction wavefront is smaller, more circular and has a higher maximum intensity than the circle of least confusion made without wavefront shaping.

Figure 2.9 shows the cross-sections of (a) the focus made by the converging spherical wavefront (b) the focus made by the correction wavefront. We can see that the focus made by the correction wavefront is smaller than the circle of least confusion made by the spherical wavefront. Also, the maximum intensity of the focus has increased compared to the circle of least confusion. To quantify the enhancement, we compare the Strehl ratios S_{before} and S_{after} and compare the resolution of the imaging systems.

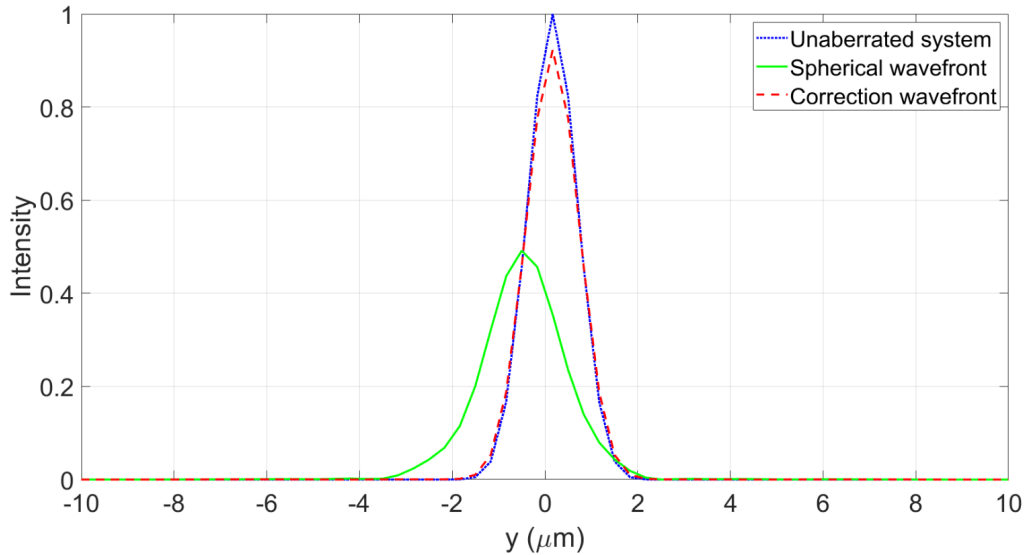


Figure 2.10: Normalized intensity in a cross-section through the focus before and after applying the correction wavefront. The Strehl ratios are calculated relative to an unaberrated system, which is the simulation of the focus of the microscope objective in water.

Figure 2.10 shows the normalized intensity as a function of distance through the simulated foci. The focus of the microscope in water has the highest intensity because there is no aberration caused by a sample. The focus without correction has a lower intensity and a larger spot size, because light is aberrated by the sample. It is also slightly off-center, because the structure is not perfectly cylindrical and the tube is not exactly in the center.

One might expect that the focus made with the correction wavefront should result in the exact same focus of an unaberrated system, because we back propagate the phase conjugate of the scattered field. However, absorbing boundaries are added in the simulation to prevent the field from wrapping around the edges due to the use of a fast Fourier transform. Therefore, some information about the aberration is lost and the wavefront cannot compensate for all aberrations.

The circle of least confusion made by the spherical wavefront has a lateral resolution of $1.85 \mu\text{m}$, while the focus made with the correction wavefront has a lateral resolution of $1.33 \mu\text{m}$. The unaberrated system has a lateral resolution of $1.25 \mu\text{m}$. Model-based wavefront shaping has improved the lateral resolution of the system by 1.4x. Using the maximum intensities in Fig. 2.10 in Eq. 2.4 and Eq. 2.5, we calculated $S_{\text{before}} = 0.49$ for the setup without correction and $S_{\text{after}} = 0.92$ for the system with correction, respectively. When the correction is applied, the system can be considered diffraction-limited. According to this simulation, model-based wavefront shaping can offer a 1.8x improvement of the Strehl ratio for the PDMS sample. Because in the experiment we use a TPM, the amount of enhancement we can expect is squared of the enhancement in the simulation [15]. This means that the maximum intensity in the experiment can theoretically become $1.8^2 = 3.2\text{x}$ higher using wavefront shaping.

2.3.3 Collagen sample

Simulating spherical wavefront through the collagen sample

We begin by simulating the focus at the bottom of the tube made with a spherical wavefront, see Fig. 2.11. The spherical wavefront has an opening angle corresponding to the microscope objective. The refractive index distribution of the tube used in this simulation is shown in Fig. 4.7b. We follow the reverse order of the propagation steps described in subsection 2.2.2, starting at plane P_5 and propagating through the tube to form a focus at the bottom of the tube.

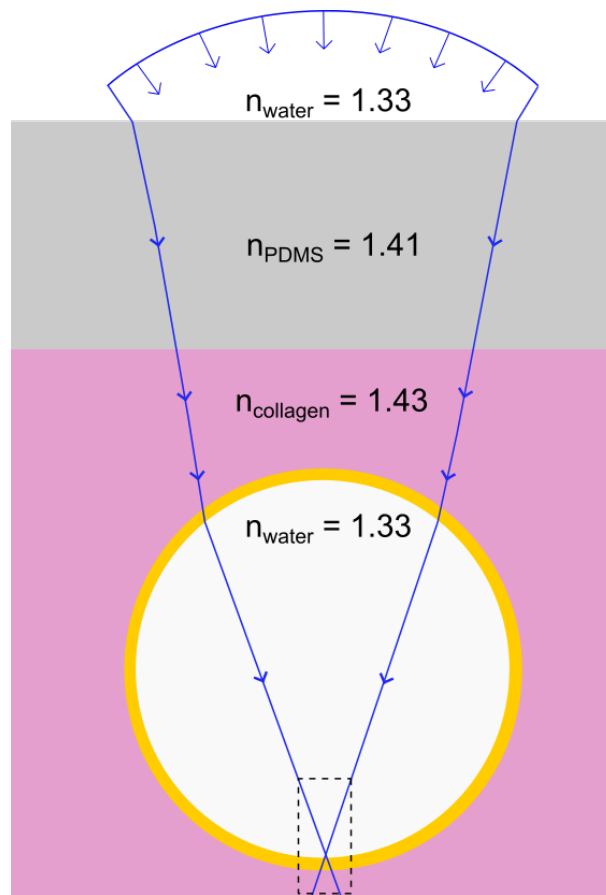


Figure 2.11: Illustration of the cross-section of the collagen sample. The dashed box indicates the region of the beam shown in Fig. 2.12.

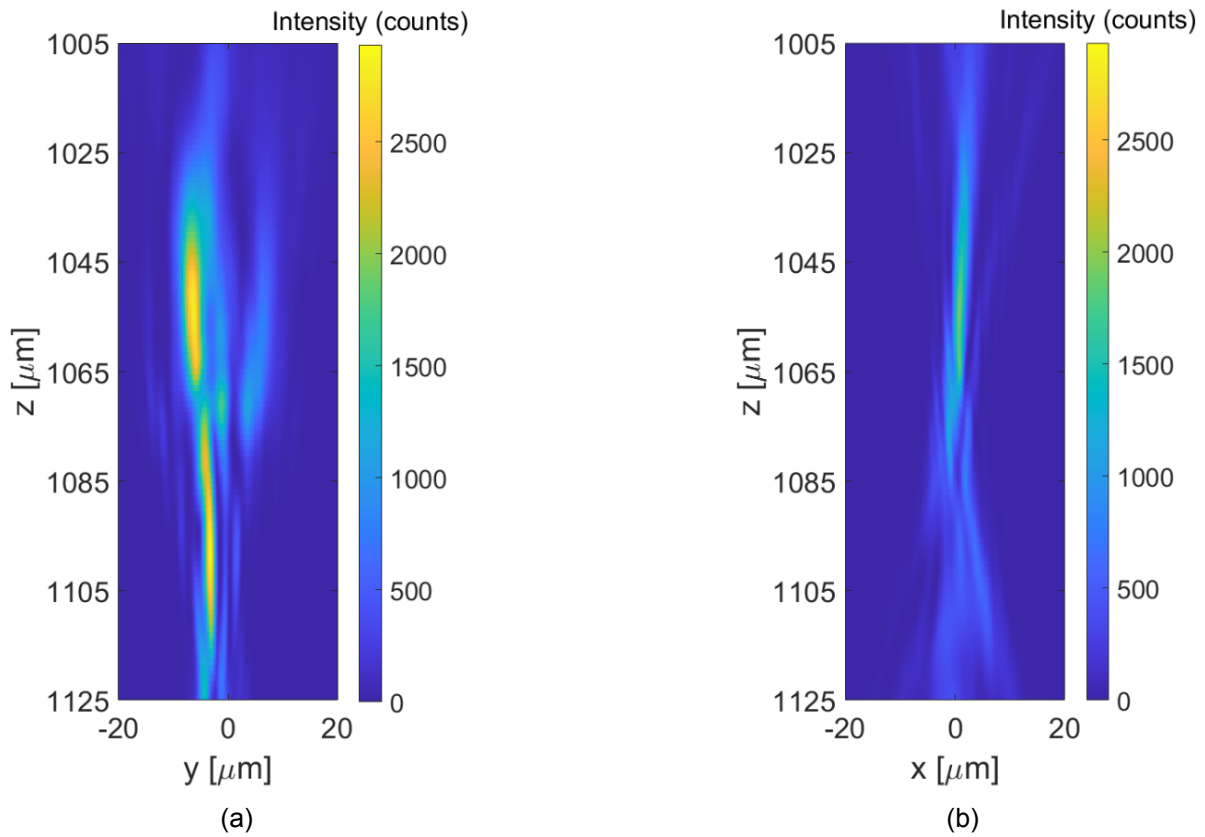


Figure 2.12: Result of simulating the focus made with a spherical wavefront through the collagen sample. The beam becomes heavily distorted due to the sample. The circle of least confusion is found at 1085 μm below the surface of the sample (a) yz plane (b) xz plane.

Figure 2.12 shows cross-sections of the focus made by simulating the propagation of the spherical wavefront through the collagen sample. We can see that the focus is heavily aberrated by the sample, because the light is not focused into a spot. Both imaging planes have a different position of their focus, caused by astigmatism from the cylindrical shape of the tube. The circle of least confusion is found at a depth of 1085 μm below the top surface of the sample. We calculate a lateral resolution of 6.27 μm based on the FWHM of the green solid curve in Fig. 2.16. The Strehl ratio of this system is calculated using Eq. 2.4 and is found to be $S_{\text{before}} = 0.06$.

Simulating virtual phase conjugation experiment through the collagen sample

We follow the modeling steps described in subsection 2.2.2 sample to calculate the aberrated field $E_5(x, y)$. The virtual point source is placed at $1085 \mu\text{m}$ below the surface, the depth where we found the circle of least confusion when using the spherical wavefront. We model the light propagation through the sample towards plane P_5 to find the phase of the correction wavefront, shown in Fig. 2.13.

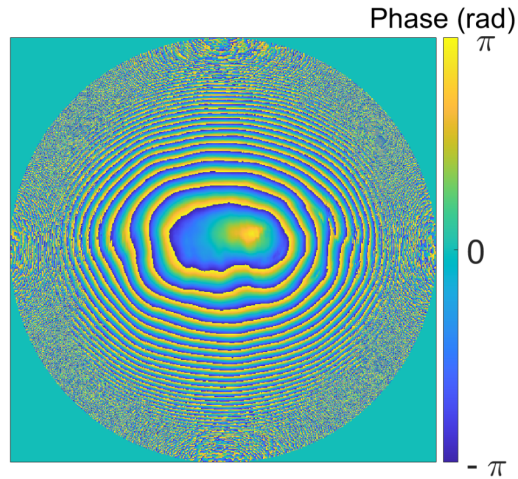


Figure 2.13: The calculated wavefront correction to focus light in the center of the tube of the PDMS sample. The size of the circle corresponds to the pupil of an objective with $\text{NA} = 0.8$.

We take the phase conjugate of the aberrated field $E_4(x, y)$ and propagate it back through the sample to find the focus made with the correction wavefront. Figure 2.14 shows a cross-section of the focusing beam, as a result of propagating the correction wavefront through the collagen sample.

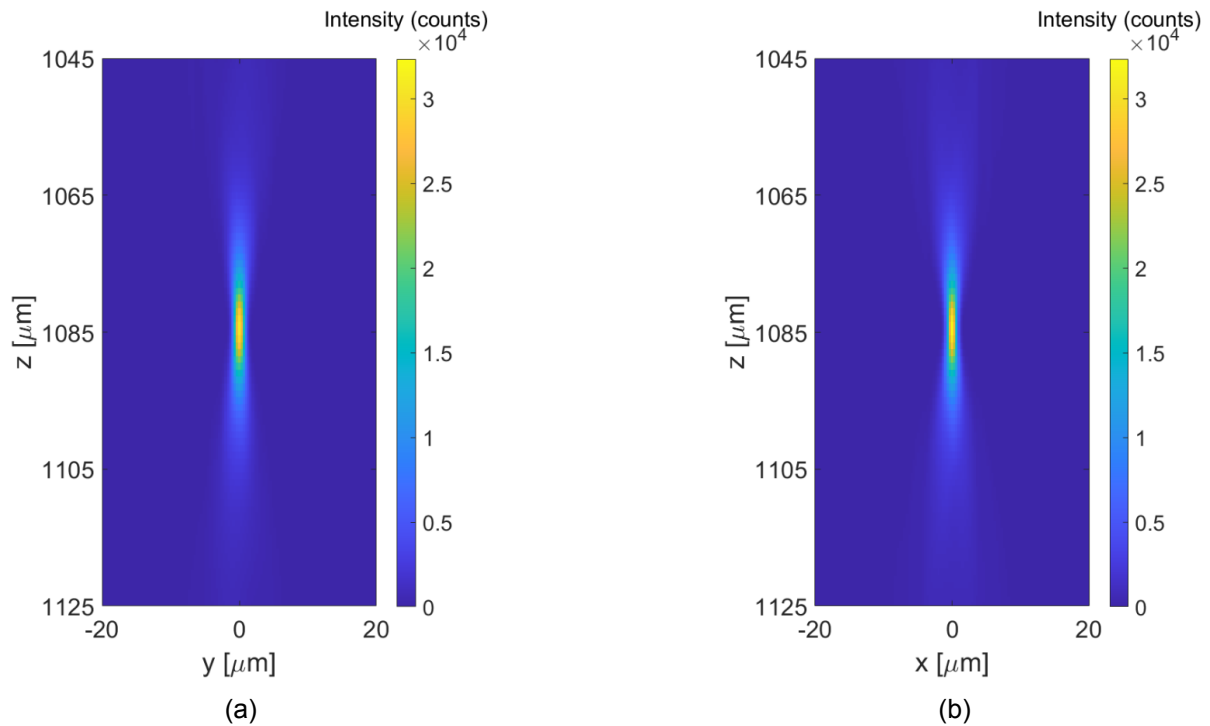


Figure 2.14: Result of simulating the focus made with the calculated wavefront correction through the collagen sample. The correction wavefront forms a focus at 1085 μm below the surface (a) yz plane (b) xz plane

When we compare figure [2.12](#) and [2.14](#), we can clearly see an improvement of the maximum intensity in the focus. The light is no longer distorted but forms a single focus, meaning that the correction wavefront corrected for the aberrations and astigmatism caused by the tube. For the system after applying wavefront shaping, we calculate a lateral resolution of 1.34 μm based on the FWHM of the red dashed curve in Fig. [2.16](#) and a Strehl ratio of $S_{\text{after}} = 0.81$ using Eq. [2.5](#).

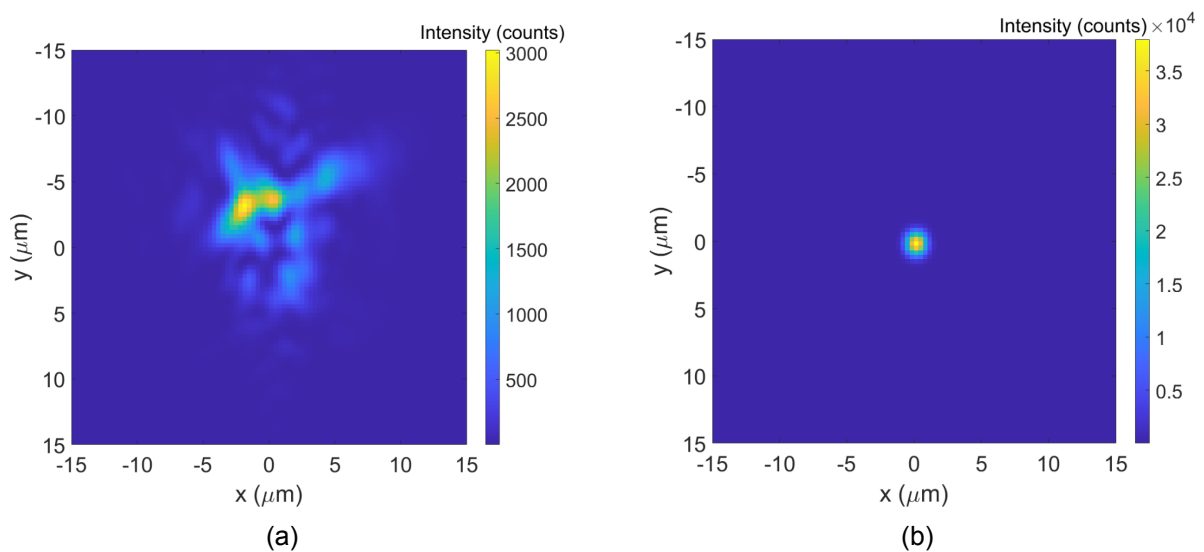


Figure 2.15: Cross-section of (a) the circle of least confusion made by a spherical wavefront (b) the focus made by correction wavefront. The focus made with the correction wavefront is smaller, more circular and has a higher maximum intensity than the focus made without wavefront shaping.

Figure 2.15 shows the cross-sections of (a) the circle of least confusion made by the converging spherical wavefront (b) the focus made by the correction wavefront. The spot size of the focus made by the correction wavefront is smaller and has a higher intensity than the cross-section of the circle of least confusion of the converging spherical wavefront. To quantify the improvement, we compare the Strehl ratios S_{before} and S_{after} and the lateral resolutions of the systems.

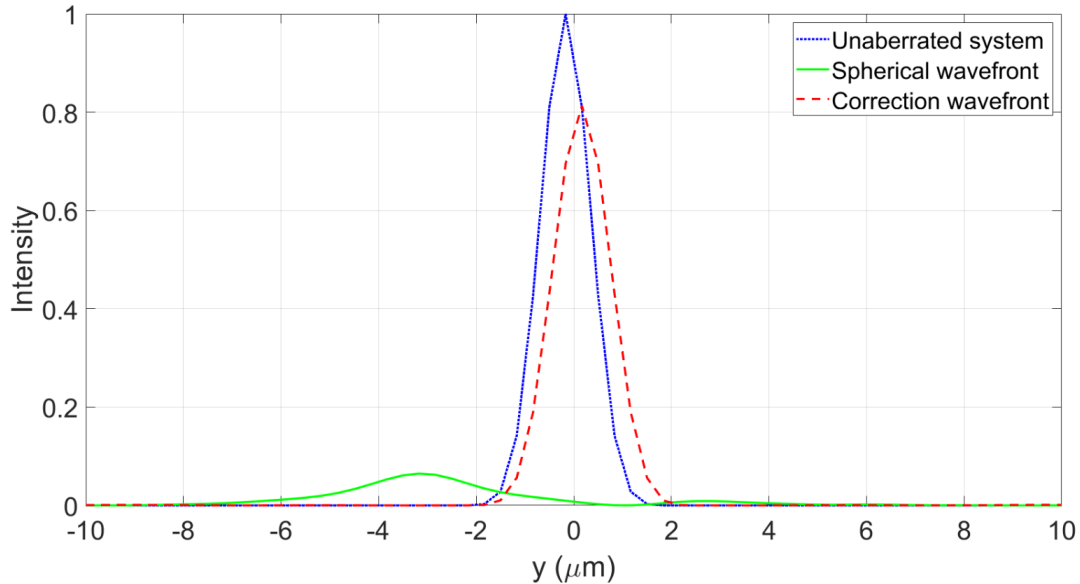


Figure 2.16: Normalized intensity in a cross-section through the focus before and after applying the correction wavefront. The Strehl ratios are calculated relative to an unaberrated system, which is the simulation of the focus of the microscope objective in water.

Figure 2.16 shows the intensity as function of distance through the simulated foci. The intensities are normalized to the intensity of the unaberrated system. We measured the FWHM of the three curves to find the lateral resolution for each system. The focus without correction has a lateral resolution of $6.27 \mu\text{m}$, while the focus with the correction has a lateral resolution of $1.34 \mu\text{m}$ and the unaberrated system has a lateral resolution of $1.25 \mu\text{m}$. Model-based wavefront shaping has improved the lateral resolution of the system 4.5x. Using the maximum intensities in Fig. 2.16 in Eq. 2.4 and 2.5, we calculate $S_{\text{before}} = 0.06$ for the setup without correction and $S_{\text{after}} = 0.81$ for the system with correction, respectively. This means a significant 13x improvement of the Strehl ratio. In the experimental setup using the TPM, this translates to a $13^2 = 169\text{x}$ higher maximum intensity.

3 EXPERIMENTAL

3.1 Setup

The experimental setup used for model-based wavefront shaping is a two-photon fluorescence excitation microscope (TPM), illustrated in Fig. 3.1. A pulsed titanium-sapphire laser (Spectra-Physics, Mai Tai) is used as a light source for two-photon excitation at wavelengths of 804, 850 and 855 nm. A combination of a half-wave plate (HWP) and a polarizing beam splitter (PBS) control the power and the polarization of the light. The laser beam is expanded 10x and sent to two galvo mirrors (GM, Thorlabs, GVS111) which scan the beam in two lateral directions x and y . A spatial light modulator (SLM, LC, Meadowlark Optics, 1920×1152 pixels) is used to modulate the phase of the light and is conjugated to the pupil plane of the objective lens (Nikon, CFI75 LWD 16x/NA 0.8). The objective is mounted to a piezo scanning stage (PI, PD72Z2x/4x) for depth scanning. A photomultiplier tube (PMT, Hamamatsu, H10770(P)A-40/-50) is used to collect the fluorescent and second-harmonic signals from the sample. To filter out unwanted signals, a dichroic mirror (DM, Semrock, FF685-Di02-25 \times 36) and a short pass transmission filter (SPF, Semrock, FF01-680/SP-25, FF01-520/44-25, FF01-427/10-25) are used depending on the wavelength that is emitted. The sample is placed on a 3D stage to easily navigate through the sample, and to measure the thicknesses of the materials in the sample.

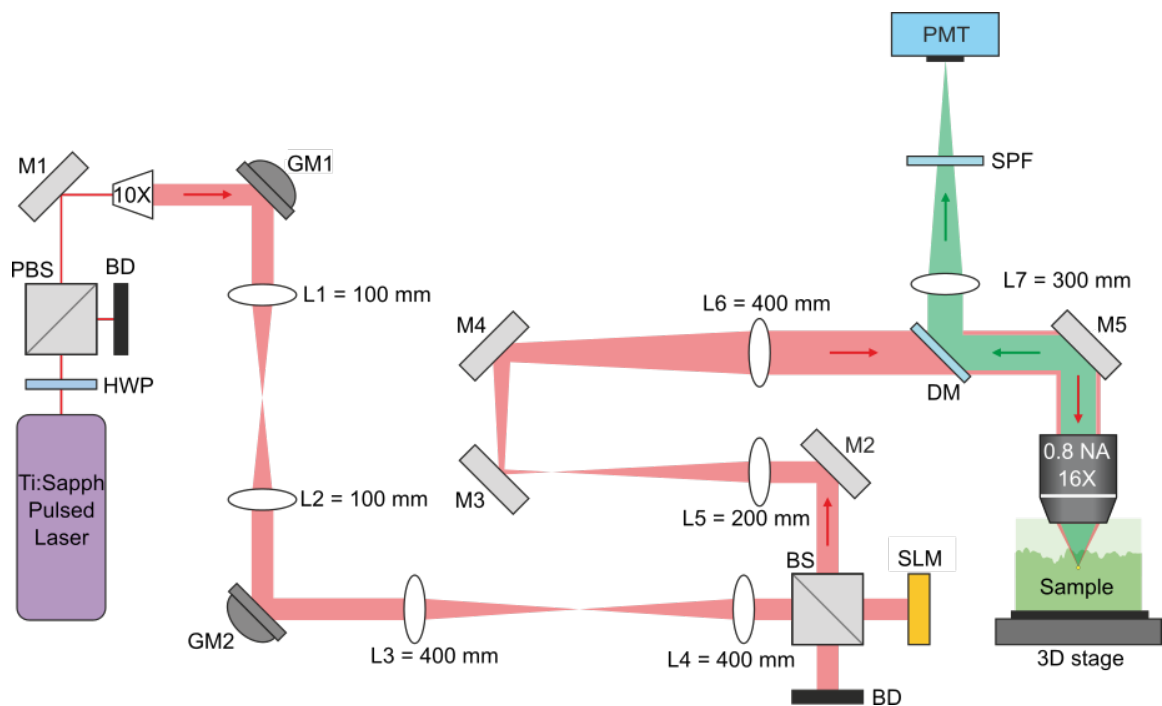


Figure 3.1: Experimental setup for two-photon fluorescence excitation microscopy. HWP, half-wave plate, PBS, polarizing beam splitter, M, mirror, GM, galvo mirror, L, lens, BS, 50/50 beam splitter, BD, beam dump, SLM, spatial light modulator, DM, dichroic mirror. Image reproduced from [7].

3.2 Sample preparation

The lung-on-a-chip samples were provided by the Applied Microfluidics for BioEngineering Research (AMBER) group following the fabrication protocols included in Appendix B - D. The samples consist of polydimethylsiloxane (PDMS), collagen I (Corning, high concentration, rat tail - 0.02 N in acetic acid) and 16-HBE14o human bronchial epithelial cells. A 300 μm diameter nylon monofilament is inserted in the holes of a 3D-printed mold. A 1:10 ratio of PDMS molding and Sylgard 184 curing agent is poured and degassed on the mold. Excess PDMS is removed before curing it. The nylon monofilament is removed before the PDMS cast is taken out of the mold. A 250 μm diameter stainless steel filament is partially placed in the outlet of the PDMS cast. The chips are kept on ice before injecting the collagen with the cell culture in the central reservoir. The steel filaments are moved into the central reservoir to the vertical inlets, which creates a hollow tube. The samples are incubated before removing the steel filaments and immersing it in phosphate buffered saline (PBS).

3.3 Measurement procedure

The sample is placed on a 76x26x1 mm microscope slide. For the PDMS sample, fluorescein dye (Sigma-Aldrich) is injected in the tube to act as a contrast agent. For the collagen sample, we use the second harmonic properties of collagen to differentiate between the inside and outside the tube. Since additional staining is unnecessary, we inject demi-water into the tube. The sample is placed in the TPM. A drop of fluorescein dye is placed on the top of the sample to visualize the PDMS-water interface. The first step is to obtain a 3D image of the upper half of the tube. For the PDMS sample, the wavelength of the laser is set at 804 nm corresponding to the excitation wavelength for which the emission of fluorescein is the highest. We used a Semrock FF01-680/SP-25 filter to prevent the laser light from reaching the PMT. For the collagen sample, the excitation wavelength is set to 855 nm, and we use a Semrock FF01-427/10-25 filter to receive only the second harmonic signal from the collagen. We obtain a stack of images of the upper part of the tube. This 3D image is used to reconstruct a digital refractive index distribution of the upper part of the tube. The procedure of the reconstruction is explained in Section 4.1 and 4.2 for the PDMS sample and collagen sample, respectively. To model the light propagation through the samples, it is necessary to know the thickness of each simulation volume. For the PDMS sample, we need to measure only the thickness d_3 of the PDMS layer, see Fig. 2.2. For the collagen sample, we need to measure the thickness d_3 of the collagen layer and d_4 of the PDMS layer, see Fig. 2.3.

Figure 3.2 illustrates the general concept of measuring the thickness of a simulation volume. The thickness of the volume is measured by moving the sample stage until the bottom plane of the simulation volume P_{z1} is in focus, see Fig. 3.2a. We write down the coordinates displayed on the sample stage and move the sample stage until the top plane of the simulation volume P_{z2} is in focus, as illustrated in Fig. 3.2b. The coordinates on the sample stage are written down and subtracted to find the distance d' between the two surfaces. Because the microscope objective is designed to be water-immersed, the measured distance d' is shorter than the actual distance d by a factor $\frac{n_2}{n_1}$. This effect is due to refraction at the P_{z2} interface, as illustrated in Fig. 3.2a. The distance used in the light propagation model is the distance $d = \frac{n_2}{n_1} d'$ in Fig. 2.2 and 2.3.

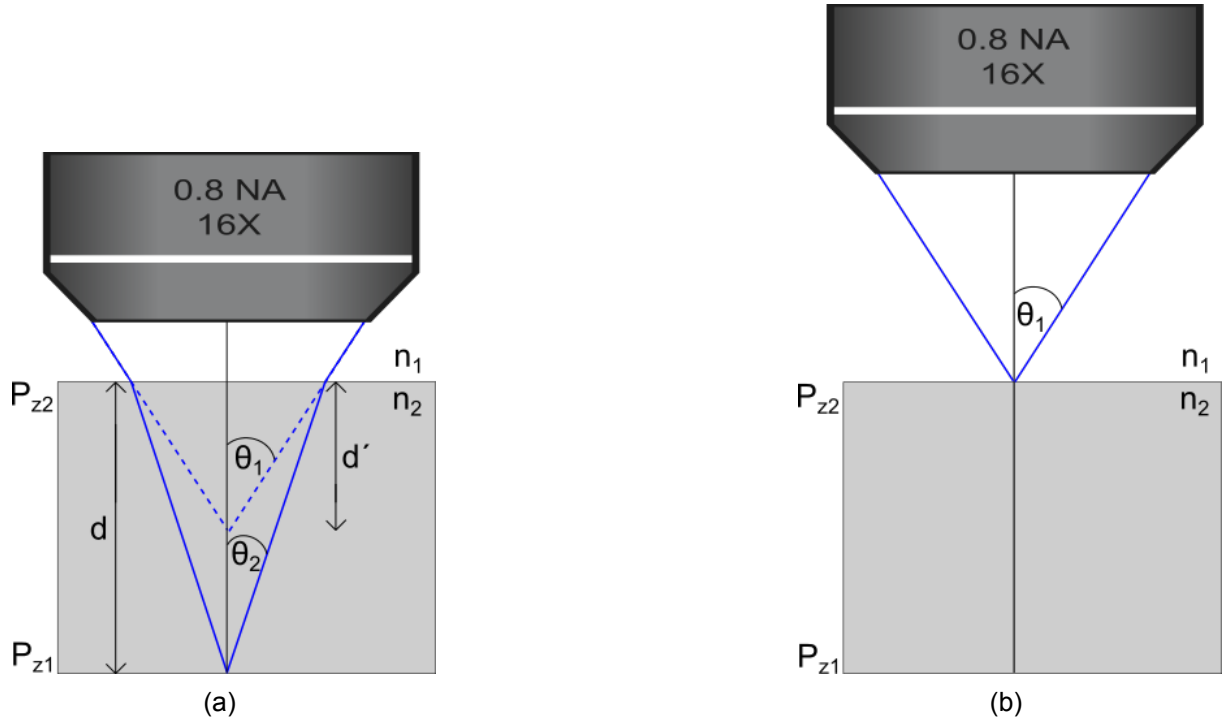


Figure 3.2: General concept of measuring the simulation volume thicknesses (a) The sample stage is moved until plane P_{z1} is in focus. (b) The sample stage is moved until plane P_{z2} is in focus. Due to refraction the measured distance d' is shorter than the actual distance d . Therefore, d' is multiplied by a factor $\frac{n_2}{n_1}$ to get the geometrical distance d .

For the PDMS sample, we measure the thickness of the simulation volume for PDMS from plane P_2 to P_3 , see Fig. 2.2. The top interface of the sample is in focus when we receive the bright signal from the fluorescein. For the collagen sample, we first measure the thickness d_3 of the collagen layer, by measuring the distance between plane P_2 and P_3 , see Fig. 2.3. The collagen-PDMS interface is visualized by the transition from high signal of collagen to no signal from PDMS. After that, we measure the thickness d_4 of the PDMS volume from plane P_3 to P_4 . To visualize the top interface, the excitation wavelength is changed to 804 nm for fluorescein and the filter is switched to the Semrock FF01-680/SP-25 filter. With the distances measured, the digital refractive index distribution of the sample is reconstructed and the wavefront correction can be calculated, see Section 2.2 for the calculation steps.

When the correction wavefront is calculated, we apply the correction on the SLM and move the microscope objective to the location of the virtual point source. For the PDMS sample, the center of the tube is imaged without correction and with correction to determine the enhancement of the focus. For the collagen sample, the bottom of the tube is imaged without correction and with correction to determine the enhancement of the focus.

4 EXPERIMENTAL RESULTS

In Section 2.3 we calculated the theoretical increase of the maximum intensity based on a simulation of the experiment. This chapter presents and discusses the results of the phase conjugation experiment using the experimental setup and measurement procedure described in Chapter 3. The results of the PDMS sample and collagen sample are separately discussed in Section 4.1 and 4.2 respectively. The results of the experiment are compared to the results of the simulation.

4.1 Experimental results: PDMS sample

For the PDMS sample, the fluorescein in the tube generates a uniform signal when we excite it with the laser light. In this experiment, we aim to improve the focus in the middle of the tube, 892 μm below the surface of the sample. Because light is focused in a bulk of fluorescein, we expect to receive a uniform signal from the fluorescein throughout the tube. After applying the correction, we expect to receive a higher intensity in one area of the sample and a lower intensity in other areas, because of the improved focus. According to the simulations, we can expect a maximum increase of 3.2x the intensity. The imaging region is indicated by the black rectangular dashed box in Fig. 4.1. First we image this region using conventional TPM imaging, to measure the signal strength of the fluorescein without correction.

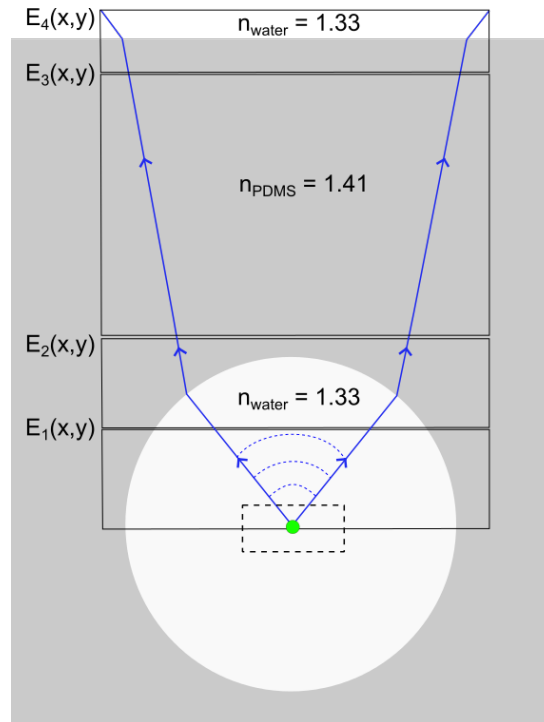


Figure 4.1: Schematic cross-section of the PDMS sample to illustrate where the light is focused. The region in the tube where the focus is optimized is indicated by the black dashed box.

Figure 4.2 shows a 2D cross-section of a stack of images acquired at the focus created with conventional TPM. The stack of images consists of 60 frames of 512x512 pixels with a spacing of 1 μm to acquire a volume of 160x160x60 μm^3 . The signal in Fig. 4.2 is coming from the fluorescein in the tube.

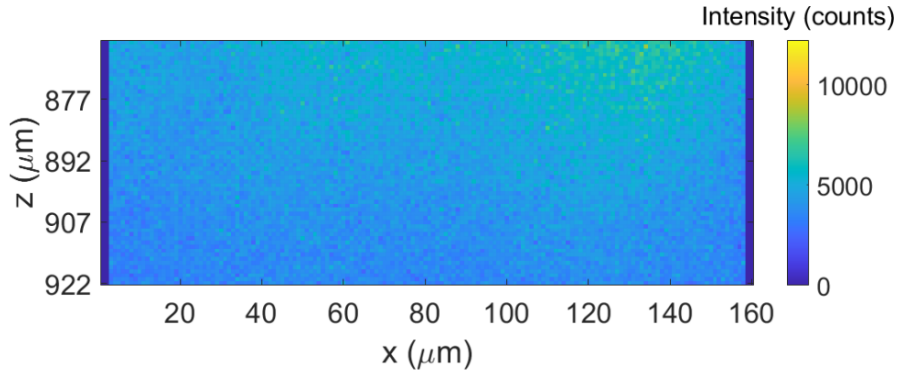


Figure 4.2: Cross-section of the focus made with conventional TPM imaging.

To calculate the correction wavefront, we need the refractive index distribution of the upper part of the tube as input for our model of the sample. We used the TPM to image the upper part of the PDMS-water interface of the tube. The tube is filled with fluorescein dye to distinguish the inside of the tube from the surrounding PDMS. We obtained a stack of 50 frames of 512x512 pixels with a spacing of 1 μm to acquire a volume of 200x200x50 μm^3 . Figure 4.3a shows a 2D cross-section of the middle frame from the stack of TPM images. The bright semicircular shape is the high intensity from the fluorescein in the tube, the low intensity area is the lack of fluorescent signal coming from PDMS. The quality of the image could be improved by lowering the gain and increasing the laser power to increase SNR. A median filter of 9x9x9 voxels is applied to filter noise from the image. By inspecting the filtered image, a threshold value is chosen which is used to assign the appropriate refractive index to each part. Intensity values above the threshold correspond to a refractive index of water, while intensity values below the threshold value correspond to a refractive index of PDMS. To further smooth the refractive index distribution, a smooth filter of 15x15x15 voxels is used. The reconstructed refractive index distribution of the PDMS sample is shown in Fig. 4.3b. This is the same refractive index distribution that we used in the simulation in Subsection 2.3.2.

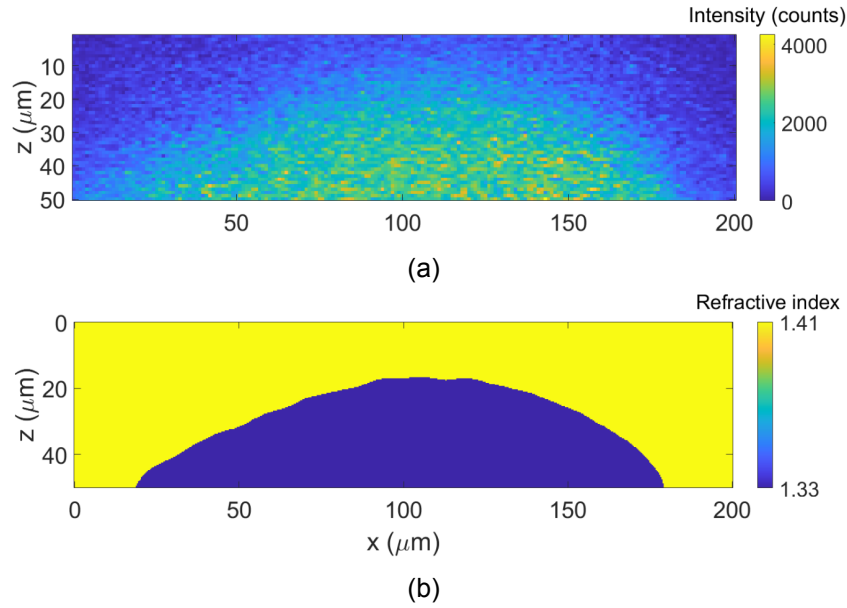


Figure 4.3: (a) 2D cross-section of the acquired TPM images of the water-PDMS interface of the upper half of the tube. (b) Reconstructed refractive index distribution using the TPM images.

We use the reconstructed refractive index distribution of Fig. 4.3b in the refractive index model of the PDMS sample to calculate the correction wavefront. The correction wavefront to focus light in the center of the tube is shown in Fig. 4.4. The wavefront is oval-shaped to correct for the aberrations introduced by the cylindrical shape of the tube.

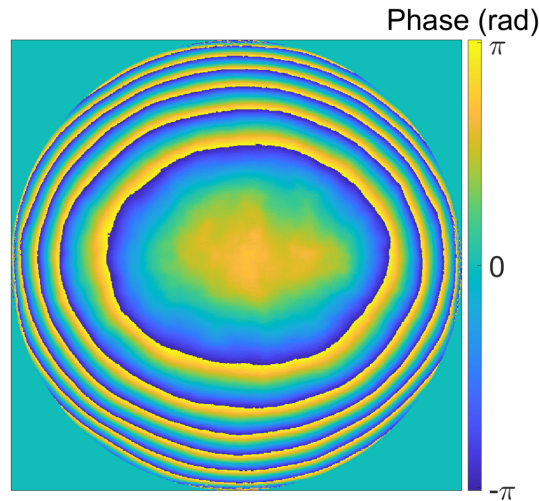


Figure 4.4: The correction wavefront used in the experiment. The size of the circle corresponds to the pupil of an objective with NA = 0.8.

The final step in the experiment is to put the calculated correction wavefront on the SLM to modulate the light. We applied the correction wavefront to the SLM and imaged the same region in the tube, as indicated by the black dashed box in Fig. 4.1. Figure 4.5 shows the intensity of the fluorescein after applying the correction wavefront. An increase of the intensity can be seen over the entire 60 μm stack. The increased intensity is a result of a better focus, because more light is exciting the fluorescein in that area. Because light is more focused in one area, other parts of the sample receive less light and thus appear darker.

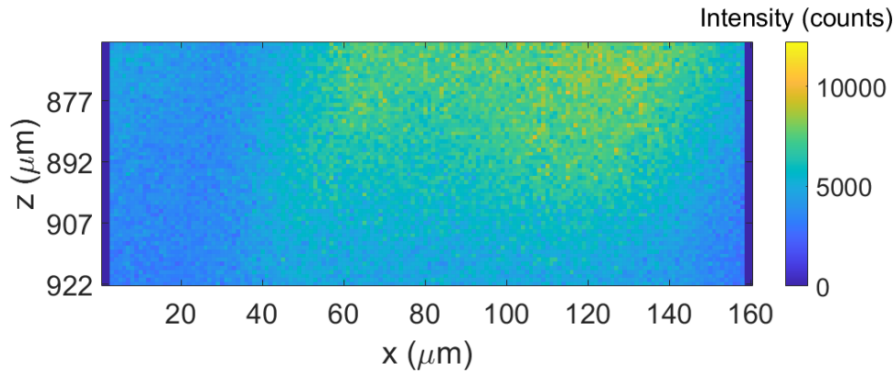


Figure 4.5: Intensity of the bulk fluorescein at the center of the tube after applying correction. The intensity at the focus has increased due to wavefront shaping.

Figure 4.6 shows the fluorescein signal as a function of depth before and after applying the correction wavefront. During the experiment, the gain of the PMT is kept constant. We notice that the intensity after correction is consistently higher than the signal before applying the correction. The intensity of the signal after correction is about 1.3x higher than the signal before applying the correction. From the simulations, we calculated that the Strehl ratio became 1.8x higher when applying the correction. Because we are using a TPM during the experiment, the amount of enhancement that we can expect is squared of that from the simulation [15]. This means that the intensity in the experiment can theoretically become $1.8^2 = 3.2x$ higher than the intensity before the correction.

We also notice that the intensities of both signals decrease as the imaging depth increases. Although we are not sure why the intensities decrease, it is suspected that it is caused by absorption of light by the fluorescein.

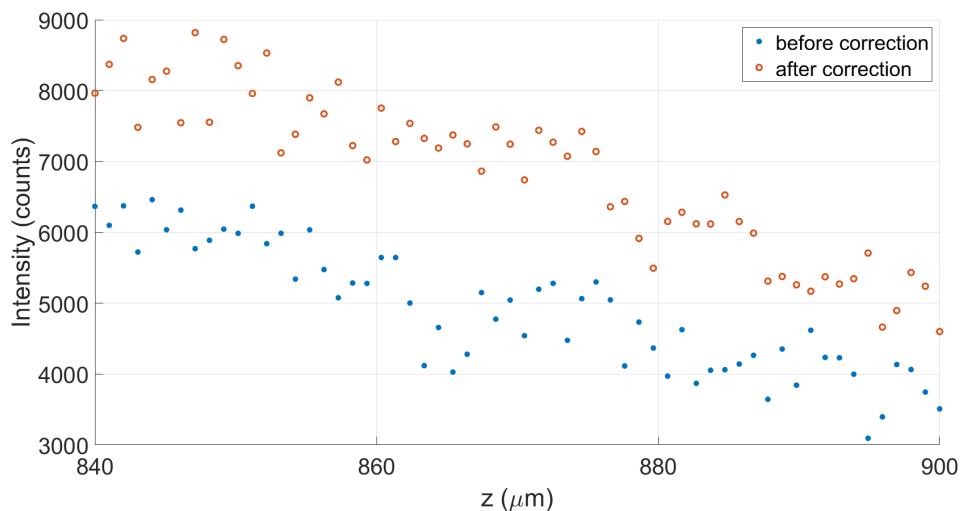


Figure 4.6: Two-photon fluorescein signal as function of depth. The blue line is the signal before applying the correction. The red line is the signal after applying the calculated correction.

The increase of 1.3x the intensity shows that model-based wavefront shaping can be used to increase the intensity in the center of the tube. Because the PDMS sample cannot be used to grow cells inside the wall of the tube, it is not an interesting sample from a biological point of view. We therefore decided to proceed with the collagen sample, since this sample can be used to investigate the uptake of nanometer-sized plastic particles.

4.2 Experimental results: collagen sample

For the collagen sample, we cannot use fluorescein to visualize the tube, because it diffuses through the collagen matrix when it is injected in the tube. Therefore, we make use of the second harmonic properties of collagen to image the tube without additional staining. Although second harmonic generation is a forward directed process, the signal received in reflection was sufficient to visualize the tube [16]. We measured the excitation spectrum of collagen in reflection, which showed the highest intensity for a wavelength of 855 nm. Because in second harmonic generation, the emitted wavelength is half of the incident wavelength, a 427/10 nm filter is used appropriate to the SHG signal of collagen. The approach for reconstructing the refractive index distribution in collagen is the same as for PDMS. We obtained a stack of 140 frames with a spacing of 1 μm to acquire a volume of $340 \times 340 \times 140 \mu\text{m}^3$. Figure 4.7a shows a 2D cross-section of the middle frame from the stack of TPM images. A median filter of $21 \times 21 \times 21$ voxels is applied to filter noise from the image. Since the high intensity is due to the second harmonic signal from the collagen and the low intensity due to the lack of signal from the water inside the tube, values above and below the threshold value are assigned the refractive index of collagen (1.43) [17] or water (1.33) respectively. To further smooth the refractive index distribution, a smooth filter of $19 \times 19 \times 19$ voxels is used. The reconstructed refractive index distribution of the upper half of the tube is shown in Fig. 4.7b. This is the same refractive index distribution that we used in the simulation of the collagen sample in Subsection 2.3.3.

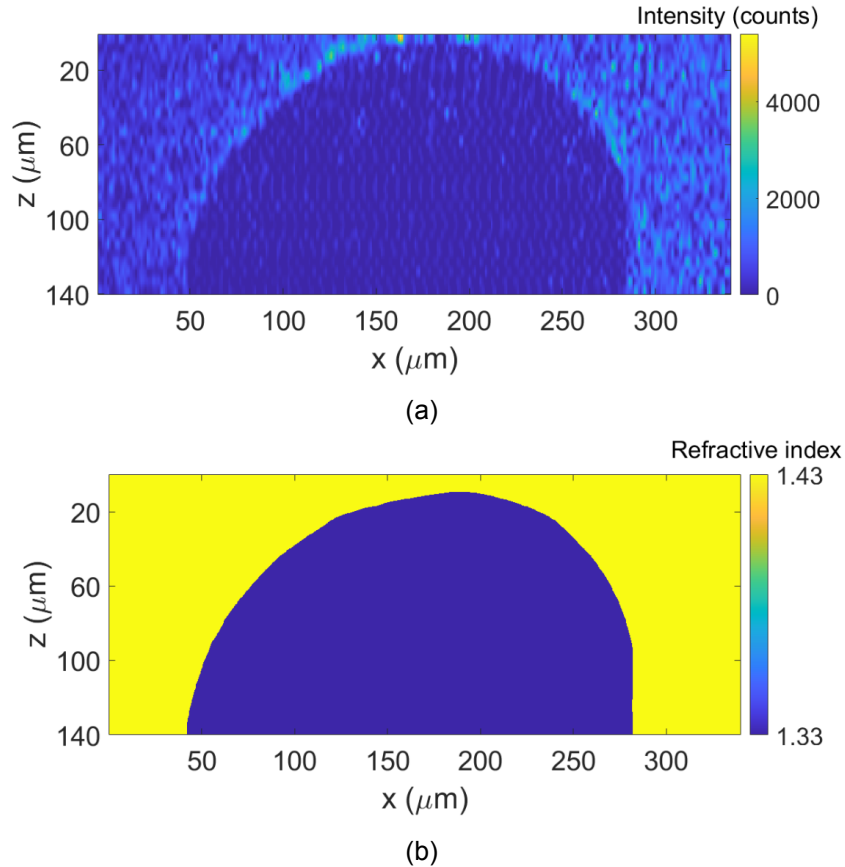


Figure 4.7: (a) 2D cross-section of the acquired TPM images of the water-collagen interface of the upper half of the tube. (b) Reconstructed refractive index distribution using the TPM images.

We calculated the correction wavefront and found the wavefront presented in Fig. 4.8. In the simulation, we saw that the Strehl ratio improved 13x when using this correction. Because the intensity in the experiment is squared of the intensity in the simulation [15], the intensity in the experiment can theoretically become 169x higher using model-based wavefront shaping. Unfortunately the calculated wavefront could not be tested because at the time the TPM microscope was moving to a different laboratory space.

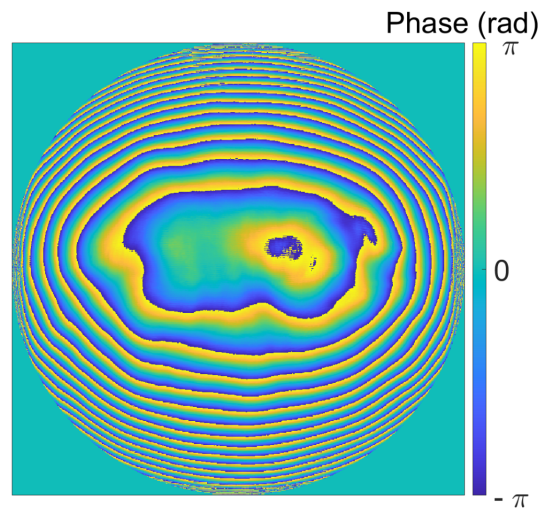


Figure 4.8: The calculated SLM pattern to focus light at the bottom of the tube. The size of the circle corresponds to the pupil of an objective with $NA = 0.8$

5 CONCLUSION AND RECOMMENDATIONS

With this research we showed for the first time that model-based wavefront shaping can be used to improve the focus inside a large 3D structure such as a lung-on-a-chip device. We used two samples, the PDMS sample and the collagen sample. For both samples, we reconstructed a 3D refractive index distribution of the sample using a stack of images obtained with the TPM. For the collagen sample, we managed to image the aberrating surface inside the sample without using additional staining, by utilizing the second harmonic properties of collagen. We calculated the theoretical enhancement by performing a simulation of the experiment. The results are quantified using the Strehl ratio and the FWHM of the intensity in the cross-section of the focus.

For the PDMS sample, we found a theoretical improvement of 1.8x for the Strehl ratio and a 1.4x increased lateral resolution when using model-based wavefront shaping. Since we used a two-photon microscope for the experiment, the intensity in the experiment is squared of the intensity in the simulation, which means that we could expect a 3.2x higher intensity at most during the experiment. Experimentally, we found an increase of about 1.3x the intensity in a bulk of fluorescein in the tube of the PDMS sample. For the collagen sample, we simulated a 13x increase of the maximum intensity in the focus when using model-based wavefront shaping. This translates to a 169x higher intensity when using the two-photon microscope during the experiment. Unfortunately, the calculated wavefront could not be tested experimentally, because the two-photon microscope was moved to a laboratory suited for live-cell imaging.

A point of improvement would be to find a way to automate the choosing of the threshold value when reconstructing the refractive index distribution of the tube. So far, the threshold value is manually chosen, which is less robust and slows down the experiment. Edge detection could be used to find the interface between the tube and the surrounding material, after which the refractive indices can be assigned.

With the experimental setup moved to the Live Cell Imaging Facility, the next step is to use the calculated correction wavefront for the collagen sample in an experiment. If we can improve the focus at the bottom of the tube, the next step would be to image cells at the bottom of the tube. If we can successfully image cells, model-based wavefront shaping can very well become the solution to finally being able to perform real-time live cell imaging in organ-on-a-chip devices and could mean that soon animal testing could become a relic of the past.

Bibliography

- [1] D. Huh, B. D. Matthews, A. Mammoto, M. Montoya-Zavala, H. Y. Hsin, and D. E. Ingber. Reconstituting Organ-Level Lung Functions on a Chip. *Science*, 328(5986):1662–1668, June 2010.
- [2] J. M. Wilkinson. Need for alternative testing methods and opportunities for organ-on-a-chip systems. In *Organ-on-a-chip*, pages 1–11. Elsevier, 2020.
- [3] I. M. Vellekoop and A. P. Mosk. Focusing coherent light through opaque strongly scattering media. *Optics Letters*, 32(16):2309, August 2007.
- [4] R. Horstmeyer, H. Ruan, and C. Yang. Guidestar-assisted wavefront-shaping methods for focusing light into biological tissue. *Nature Photonics*, 9(9):563–571, September 2015.
- [5] G. Osnabrugge, R. Horstmeyer, I. N. Papadopoulos, B. Judkewitz, and I. M. Vellekoop. Generalized optical memory effect. *Optica*, 4(8):886, August 2017.
- [6] <https://www.utwente.nl/en/tnw/bmpi/research/wavefront-shaping/>.
- [7] A. Thendiyammal, G. Osnabrugge, T. Knop, and I. M. Vellekoop. Model-based wavefront shaping microscopy. *Optics Letters*, 45(18):5101, September 2020.
- [8] B. Y. Zel'Dovich, N. F. Pilipetsky, and V. V. Shkunov. *Principles of Phase Conjugation*. Springer Series in Optical Sciences. Springer-Verlag, Berlin Heidelberg, 1985.
- [9] <https://github.com/IvoVellekoop/bpm>.
- [10] J. W. Goodman. *Introduction to Fourier Optics*. W. H. Freeman, May 2017.
- [11] X. Cheng, Y. Li, J. Mertz, S. Sakadžić, A. Devor, D. A. Boas, and L. Tian. Development of a beam propagation method to simulate the point spread function degradation in scattering media. *Optics Letters*, 44(20):4989, October 2019.
- [12] E. Hecht. *Optics*. Pearson Education, Inc, Boston, 5 ed edition, 2017.
- [13] F. L. Pedrotti and L. S. Pedrotti. *Introduction to Optics*, volume 3 ed. Prentice Hall, 2014.
- [14] J. Kubby, S. Gigan, and M. Cui. *Wavefront Shaping for Biomedical Imaging*. Cambridge University Press, 2019.
- [15] J. R. Lakowicz. *Principles of fluorescence spectroscopy*. Springer, New York, 3rd ed edition, 2006.
- [16] R. W. Boyd. *Nonlinear Optics*. Academic Press, 3 ed edition, May 2008.
- [17] X. J. Wang, T. E. Milner, M. C. Chang, and J. S. Nelson. Group refractive index measurement of dry and hydrated type I collagen films using optical low-coherence reflectometry. *Journal of biomedical optics*, 1(2):212–216, April 1996.

A PROTOCOL: IMAGING LUNG-ON-A-CHIP WITH TPM

by Merle van Gorsel

Equipment:

- lung-on-a-chip sample
- 76 x 26 x 1 mm microscope slide
- fluorescein solution
- pipette
- tissue papers to clean up
- Optical filters:
 - 427/10 nm for collagen type 1
 - 520/44 nm filter for labeled nanospheres in tube
 - 680 nm rejects the laser light

Matlab code used: Folder: git \loc
In order of appearance:

1. Scanimage.m
2. PrepareTPMimage_OoC.m
3. Refractive_indexmap_collagen.m
4. Model_WFS_Simulation_collagen.m
5. in folder: git\setup\setup.m
6. WFScomparison_OoC.m

This imaging protocol is an extension to the measurement protocol of the 2 photon microscope last modified by Abhilash Thendiyammal. For completeness the parts of that measurement protocol that are needed are included here as well.

Let's get started:

Close the door and push the green button left of the door to be able to start the laser.

Log into the lab pc and open the Mai Tai software. Choose COM4. Choose the wavelength (**855 nm** for collagen) that you want to use and **write it down**. You can turn on the laser, but keep the shutter closed.

Make sure the PMT is off and the gain is set to zero. You can check if the PMT is off by opening the lid and feel with your hand if the ventilator is on. If the ventilator is off, so is the PMT. The gain of the PMT can be set to zero by rotating the knob of the PMT all the way to the left (counterclockwise).

Select the appropriate filter for your experiment. There are 6 filters in the setup. A list of the filters currently in the setup is adhered on the inside of the lid that closes off the box where the filters are in. The datasheets of all filters are found in "P:\TNW\BMPI\Projects\WAVEFRONTSHPING\equipment\Two-Photon Microscope\Filters". check if the transmission camera is closed.



Figure A.1: Knob to change the gain of the PMT

measure the power in the reference path

Again make sure the door is closed and the PMT is turned off.

Make sure the calibrated photodiode is connected and turn it on.

Put on your safety glasses.

Open the shutter of the laser by pressing the shutter icon in the MaiTai software for three seconds.

Turn off the light in the room.

You can adjust the power by electronically rotating the halfwave plate. You do this by pressing the left or right green button. *Do not touch the halfwave plate by hand.*

Once you have a laser power of about 1W, you **write down the laser power**. The measured power is lower than the power passing through the sample. To find out the power through the sample, look up the table (formula) for this in `git/tpm/setup/setup.m`

When you're done measuring the power, turn off the shutter by clicking on the shutter icon in the MaiTai software. You can now take off your safety glasses and turn on the light if you want.

Open Matlab and run 'scanimage.m'

(P:\TNW\BMPI\Projects\WAVEFRONTSHPING\code\scanimage.git). The first pop-up is for the location of settings. Usually, you use the default settings (load default setting), so just press Continue, without changing the default location. While ScanImage is starting up, you can prepare your sample for measurement.



Figure A.2: Press the green buttons to rotate the halfwave plate.

Prepare the sample:

Take the sample and fluorescein out of the fridge. Carefully take one of the samples out of the container (do not damage the collagen). You might need to use a small tool such as tweezers or a coffee stirrer.

Using a pipette, inject some demi water into the channels using the inlet holes on either the side or the top of the sample. Remove excess water from the top surface, otherwise it will not adhere to the sample glass well enough.

Carefully place the sample bottom side up on a sample glass. The bottom side is the side that has a flat PDMS surface. Try to align the channels with either the long side or short side of the chip, as long as it is not placed diagonally.

Place the sample glass with the sample in the holder of the microscope stage. Fix the sample glass with two magnets at the ends of the sample glass.

Adjust the xy-position of the stage so that the objective is placed above the region of the sample that you want to image.

If you press down on the Z stage controller, the Z stage moves up and vice versa. The Z stage has a low/medium/high (L/M/H) speed. Set M (medium) to the Z stage (scan motor) by pressing the speed bottom. Move the stage upward towards the objective until you are as close as possible to the objective. *Be careful not to hit the objective with the sample.*

Carefully use the pipette to place a drop of fluorescein between the sample and the objective.

The measurement

Press focus in ScanImage to start measuring.

Turn off the light in the room.

Change the white level in the IMAGE CONTROL screen of the ScanImage GUI to halfway, so that the noise from the gain becomes less.

Turn on the PMT (PMT is very sensitive to light). There is a light to check whether the PMT is on, but you can also check it by opening the box with the PMT in it and feel if the fan of the PMT is on. Increase the gain of the PMT manually until you see in the IMAGE CONTROL screen of the ScanImage GUI that you have passed the big lines in the image (which means the gain is not high enough). Increase the gain even more, almost to maximum. Note: If there is too much light, you hear a click which means that the PMT turned off. If that happens, turn off the PMT and lower the gain. Wait for a few (about 3) seconds until you hear a click again. Then you can turn on the PMT again.

Put on your laser goggles. Open the shutter of the laser.



Figure A.3: Read out the power in the reference path and write it down.

To find the tube, we need to receive the second harmonic signal of collagen type 1, so select the **427/10 nm** filter.

The focus of the objective is currently below the tube, so we must move the sample stage down to find the tube.

Move out of the sample to find the tube by rotating the knob of the Z stage (use a low speed 'L'). You might need to adjust the XY position as well. To increase the refresh rate you can use 256 pixels per line.

Once you have found a nice smooth part of a tube, we need to choose a nanoparticle to focus on.

The Z position of the objective in 'MOTOR CONTROLS' must be set as close to 0 as possible, because we are later going to move it up to almost its maximum position.

Turn off the PMT before changing the filter to the **520/44 nm** filter and change the wavelength of the laser to **850 nm**.

Turn on the PMT.

Choose a particle that you want to focus on and make sure it is in the middle of your screen.

You might need to adjust XY positions of the stage or in ScanImage by pressing the blue arrows in the MAIN CONTROLS. If you used ScanImage to position the particle in the middle, **write down the 'Shift' and 'Shift Slow' values**. If for some reason you need to close ScanImage, those values are reset to zero and you are no longer focusing on the particle.

Write down the coordinate displayed on the z-stage and do not change it. At the end of the experiment you need to get back to this position to test your calculated wavefront.

Grabbing the stack of images of the tube:

Turn off the PMT before changing the filter back to **427/10 nm** and the wavelength to **855 nm**. Turn on the PMT again.

Move out of the sample using the microscope objective in ScanImage until you are halfway in the tube (the tube is at its thickest). **Write down the coordinate displayed in ScanImage.** This will be your starting point of making the refractive index map.

Move the objective upwards until you are just above the tube. **Write down the coordinate displayed in ScanImage.**

Subtract the two coordinates of ScanImage that you just wrote down to get the thickness of n_{sample} . Divide this number by 5 to get the number of slices you take (for example, $140 \mu\text{m} / 5 = 28$ slices).

Use ScanImage to move the microscope objective back to the coordinate corresponding to halfway of the tube.

In the "MOTOR CONTROLS" window of ScanImage, fill in the number of slices '# Slices' and the 'Step/Slice' is then 5.

Check the box of 'Return Home'.

Set 'Pixels/Line' to 512 and 'Zoom' to 1.

Lower the gain of the PMT until you can barely see the difference between the inside and outside of the tube.

In the 'MAIN CONTROLS', stop focusing and click the box left of 'Save'. Change the directory in which you want to save your image. In 'Basename' change the filename. The filename should at least contain the **number of pixels/line, # slices, step/slice, zoom value.**

Press 'GRAB' in the 'MAIN CONTROLS' to grab your stack of images. Wait for ScanImage to finish taking your images.

Making the refractive index map:

Open `git\loc\PrepareTPMimage.m` in Matlab.

make sure the width = 600, zoom = 1 and resZ = 5 in the code.

Press Run

A window will pop up where you can select and open the data you just saved.

Once Matlab is done a window will pop up for you to save a file called 'TPM_3D_tube.m'. Save this in the folder of your measurement.

Look at the figures and inspect if the entire upper half of the tube is clearly visible and in the middle of the frame. If not, go back to 'Grabbing the stack of images of the tube:' and readjust some parameters accordingly (depth, gain, laser power).

Open `git\loc\Collagen\Refractive_indexmap_collagen.m` (we will run this code section by section)

Make sure `f_depth` is the right value and run the '%% Parameters' section.

Load the `TPM_3D_tube.mat` file by running the next section.

Run all sections up until the '%% Median filter' section. Look at the figure and judge whether the image is smooth enough. If not, adjust the values in the square brackets and run again.

Choose a threshold value so that everything inside the tube gets assigned a refractive index of water and everything outside gets assigned the refractive index of collagen. If your initial pick

is not right, adjust the value and try again.

Run the next section with the smooth filter to further smooth the refractive index map. Adjust the convolution kernel if necessary.

Run the last two sections to see the TPM_3D_tube image alongside the refractive index distribution. **Save this image.** Also look at the volshow to see if there are any irregularities. If there are any, run the code again and adjust the threshold value and/or smooth filter order.

Finally, **Save n_sample.mat** in the folder of your measurement. **Write down the threshold value, median filter and smooth filter order** just in case.

Measuring the thickness of the collagen layer:

Move the Z-stage upwards until you see the transition between the collagen and PDMS.

Write down the coordinate displayed on the Z-stage.

From the coordinate you just measured, subtract the z-coordinate you wrote down previously. Divide this number by 10 (one step by the z-stage equals 10 micrometers) to get the distance in micrometers. From this number, subtract the thickness of the refractive index map. This distance is the thickness of the collagen layer.

Measuring the thickness of the PDMS layer:

Change the wavelength to **804 nm** and the filter to filter **680 nm** (rejects all laser light).

Move the Z-stage down until you see the interface between the PDMS layer (dark) and the fluorescein (bright).

Move the Z-stage up until you are 1.5 units (15 micrometers) below this interface.

Write down the coordinate displayed on the Z-stage.

Subtract the value corresponding to the PDMS-collagen interface from the z-coordinate corresponding to the PDMS-fluorescein interface and divide this number by 10 to get the thickness of the PDMS layer.

You can now turn off the PMT, close the shutter of the laser, turn on the light in the room and take off your glasses (*always turn off PMT before turning on the light and only take off your glasses if the shutter is closed*).

Calculating the correction wavefront:

Open git\loc\Collagen\Model_WFS_Simulation_collagen.m

In section '% Parameters to update:', fill in the f_depth, d_pdms, d_collagen and d_layer corresponding to the layer thicknesses that you measured.

In the next section, opt.lambda is the excitation wavelength of the labeled nanospheres (**850 nm**).

Press 'Run'. A window will pop up where you can load 'n_sample.mat', your refractive index distribution.

When Matlab is finished calculating, it will show a figure of the phase of the correction wavefront.

Save this figure.

Save SLMCorrection.mat

Comparing flat wavefront and correction wavefront:

run `git/tpm/setup/setup.m` to control the SLM.

Open `git\loc\WFScomparison.m`. Running either section of this code send a flat wavefront or the correction wavefront (`SLMCorrection.mat`).

Change the wavelength of the MaiTai to **850 nm** and the filter to **520/44 nm**.

Use the Z-stage to move to the coordinate you wrote down where you saw the particle.

Move the microscope objective down to its initial position as well, using ScanImage.

Put on your laser goggles

turn off the light in the room

turn down the gain of the PMT a bit before turning it on

Open the shutter of the laser

Press 'Focus' in ScanImage

If you now run either section of the `WFScomparison.m` code, you should hopefully see an improvement when you send in the correction wavefront compared to the flat wavefront.

You can use the Z-stage to move around to see how the intensity looks around the point where the enhanced focus should be.

Grab a stack of images of the situation where you send in a flat wavefront and when you send the correction wavefront.

Wrapping up the experiment:

Once you have saved the data that you want, turn off the PMT.

Turn on the laser power meter and use the half-wave plate to lower the laser power to about 10 mW, so that another user does accidentally damage their sample.

Turn off the laser power meter and close the shutter.

Take off your laser goggles and turn on the light in the room.

Lower the Z-stage and use an optics wiper to clean the objective from any fluorescein.

Use a tissue to absorb the fluorescein on top of the chip before removing the chip from the holder.

Put the chip in its container (with water) and put it away in the fridge. Clean up the appliances used and log out of the lab computer.

When you leave the compartment, press the green button next to the door to let people know the laser is no longer in operation.

And that's it, you're done :)

B FABRICATION OF MICROFLUIDIC CHIPS FOR THE LUNG-ON-CHIP PROJECT

Date: 2020-03-30

Tags:

Created by: Bastien Venzac

1 / 2

Goal : General protocol for the fabrication of the chips used in the lung and nanoplastic project

- Printing of molds: see [3D-printer protocol for PDMS mold fabrication](#). Designs: see [Microsystem designs : lung on a chip](#)

Most of the design contained a central structure with an horizontal hole in it, which sometimes continues through one of the wall of the mold. These channels need to be clean (so uncured resin is removed) before post-treatment. It's also possible that partially cured resin has to be removed with a 300µm wire before post-treatment.

For the post-treatment, UV curing during 1h and thermal treatment at 120°C during 2h is necessary for the Deep Black resin, due to the integrated channels.

- After post-treatment, 300µm diameter nylon monofilament (Piet Vogel Ziggy) was inserted inside the holes of the mold.

- PDMS molding: Sylgard 184, 1:10, poured and degassed on the mold. Excess of PDMS is removed with a game card before 60°C curing during minimum 2h. Removal of the nylon monofilament, then removal of the PDMS replica. Opening of the vertical inlets with a sharp tweezer (a thin membrane of PDMS is often present between the fishing line and the mold).

- Polydopamine coating: [Protocol : Polydopamine coating](#) , not done under sterile condition. The dopamine solution (100µl) was simply injected in the central reservoir and not pushed or pulled in the channels.

- Partial insertion of 250µm-diameter stainless steel filament (Goodfellow) inside the outlet of the PDMS replica.

- Collagen preparation: [Collagen hydrogel preparation](#)

- Chips were kept on ice before injection of 75µl of collagen in the central reservoir with a P100 pipette tip. Removal of the bubbles with a sharp tweezer. Moving the steel filaments into the central reservoir and to the vertical inlet. Injection of 2 chips (around 5min) then transfer to incubator for 30min. Removal of the stainless steel filaments and immersion in PBS or medium.

Linked item:

[Project - Lung-on-chip for nanoplastic](#)

Date: 2020-03-30

Tags:

Created by: Bastien Venzac

2 / 2



Unique eLabID: 20200330-8109bf4a67a3a772b74d0b16b1ae9798774aa179
link : <https://elabfw.utsp.utwente.nl:443/experiments.php?mode=view&id=214>

PDF generated with [elabfw](#), a free and open source lab notebook

File generated on 27-04-2020 at 13:04

C COLLAGEN HYDROGEL PREPARATION

Date: 2019-09-05

Tags:

Created by: Bastien Venzac

1 / 2

Protocol for the preparation of collagen I hydrogel.

Material :

- Collagen I HC, rat tail - 0.02N in Acetic Acid from Corning.
- PBS 10x with phenol red
- PBS 1X or cell culture medium
- NaOH 1Mol

Everything is stored in fridges.

Method:

- Keep all the products and tubes in ice during the process. Use of cold pipette tips can help but it's not necessary.

- Calculation of the volumes to mix:

C_i , C_f , V_{col} the collagen initial and final concentration and volume

V_f the final volum of collagen hydrogel

V_{PBS} the PBS 10x volume

V_{NaOH} the NaOH volume

V_b the buffer volume (demi-water, PBS 1X or medium)

$$V_{col} = V_f * C_f / C_i$$

$$V_{PBS} = V_f / 10$$

$$V_{NaOH} = 0.023 * V_{col} \quad 0.023 \text{ is the magic number linked to the pKa of collagen (to be checked)}$$

$$V_b = V_f - V_{col} - V_{PBS} - V_{NaOH}$$

Date: 2019-09-05

Tags:

Created by: Bastien Venzac

2 / 2

- First mix the PBS10X, the buffer and the NaOH
- Pipette it on top of the collagen volume. Mix vigorously with a pipette without adding any bubbles.
- Check the pH. If under 7, add more NaOH. If between 7 and 7.5, it's perfect. Above 7.5 is a problem if cells need to be added to the hydrogel.
- Transfer the collagen to the final recipient, wait at least 30min at 37°C (can be optimized).

TAADDAAA it's ready.

remarks: we had problem of gelation using MEM as buffer.



link : <https://elabftw.utsp.utwente.nl:443/database.php?mode=view&id=56>

D PROTOCOL: POLYDOPAMINE COATING

Date: 2019-06-21

Tags:

Created by: Geoffroy Gaschignard

1 / 1

Goal : To produce a Collagen gel with a target concentration of Cf, and a volume of Vf

Reactive	Polydopamine (PD)	Tris-HCl Buffer	mQ water
Masse			
Volume			

Important

- PD stains never go away !

Step:

- Prepare Tris HCl buffer (10mM, pH = 8.5)
 - Since there is no Tris HCl buffer directly available here, but there is Trizma (that is Tris)
 - So put 10mM of Tris in solution
 - Then tune the pH to 8.5 (use a pH meter for that) with HCl
- Prepare a 2 mg/mL solution of PD in Tris-HCl Buffer. This solution can't be stored, so prepare a fresh one each time.
- Load 10 μ L of PD solution in the inlet, and push it until it comes out of the outlet
- Let incubating at room temperature for 1 hour
- Perform 3-5 washes with mQ water, the same way it was done for PD solution
- Put the chip to dry for 1h at 65°C (hot plate or oven)
- The chips are ready to be used within the next three days



link : <https://elabftw.utsp.utwente.nl:443/database.php?mode=view&id=52>